1
Analytical Geochemistry

1.1
Overview of Analytical Geochemistry

In this chapter, we reconsider why we determine the concentration of elements or isotopic ratios in silicate materials. In this book, the application of analytical chemistry techniques to earth sciences is named as "analytical geochemistry."

The purposes of the analytical geochemistry are to reveal the distribution of elements and to unravel origin and evolution of the solar system including the Earth, the Moon, other planets, asteroids, dwarf planets, and comets from atomic scale to solar system scale, namely, from nanometer to tetrameter scales (the SI prefixes are summarized in Table 1.1).

It is easy to say but difficult to accomplish. In order to reach the result, we need a strategy. It took more than a century to establish five strategies in analytical geochemistry. To execute these strategies, we had to wait for developments of analytical methods. In other words, the evolution of the analytical methods was directly related to the evolution in analytical geochemistry and earth sciences. The evolution includes the new strategies to determine as many elements as possible, to measure isotopic ratios as precisely as possible, and to analyze as small an amount of the samples as possible. For example, TIMS (thermal ionization mass spectrometry) is one of the analytical methods that seemed to satisfy the requirements of analytical geochemistry. In this chapter, the strategies in analytical geochemistry are briefly reviewed.

We have five strategies in analytical geochemistry: (i) major element geochemistry; (ii) trace element geochemistry; (iii) determination of mass fractionation; (iv) age dating; and (v) radiogenic isotopes for geochemical tracers.

1.1.1
Major Element Geochemistry

When geochemistry started, the strategy was only to determine the bulk major elements using classic wet chemistry. Then the classification of rocks was the first thing we would do. For the classification of igneous rocks, the use of a TAS (total alkali versus silica) diagram was one of the most common way (see Figure 1.1).

Table 1.1 SI prefixes.

| 10^{18}	Exa	E	
10^{15}	Peta	P	
10^{12}	Tera	T	
10^{9}	Giga	G	
10^{6}	Mega	M	
10^{3}	Kilo	k	
10^{-3}	Milli	m	Empirical expression
10^{-6}	Micro	μ	$\mu g\,g^{-1} = ppm$
10^{-9}	Nano	n	$ng\,g^{-1} = ppb$
10^{-12}	Pico	p	$pg\,g^{-1} = ppt$
10^{-15}	Femto	f	$fg\,g^{-1} = ppq$
10^{-18}	Atto	a	

Empirical expressions are sometimes used, but they are not recommended.
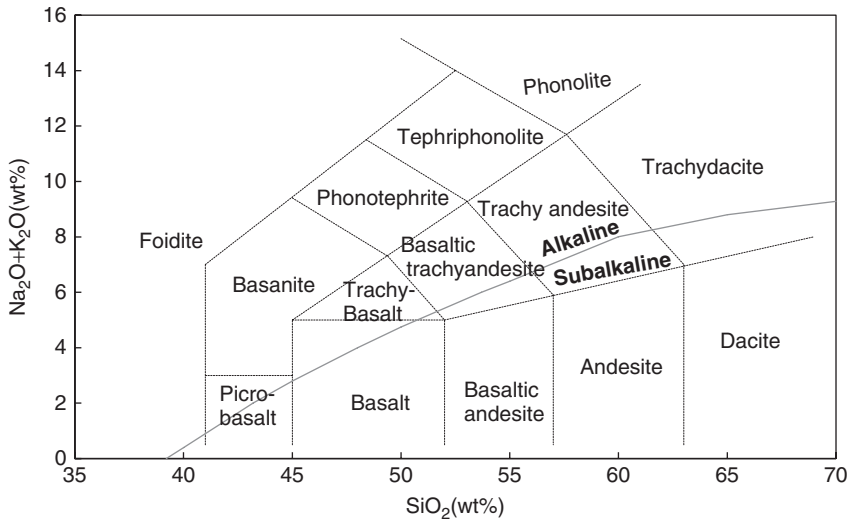
Figure 1.1 Classification of igneous rocks by SiO_2 and $Na_2O + K_2O$ abundances. The classification is after Le Maitre [8]. The discrimination line between alkaline and subalkaline is after [9].

This plots SiO_2 versus $Na_2O + K_2O$ abundances. Classifying the rocks is simple but important, but precise determination of the major elements is required.

In order to replace the time-consuming and comp lex classic wet chemistry, X-ray fluorescence spectroscopy (XRF, see Section 1.1.1.1) was invented, which has been widely used since then. Furthermore, in order to observe and determine the major elements in spot areas, secondary electron microprobe with the energy dispersive spectrometry (SEM-EDS; see Figure 1.2) and electron probe
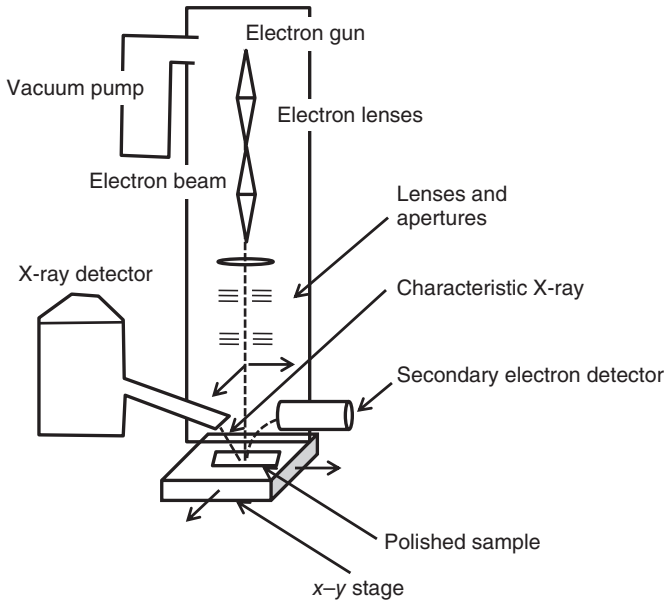
Figure 1.2 Schematic diagram of the scanning electron microscope (SEM). The electron beam is produced at the top of the column, and the shape of the electron beam is reformed using electron lenses and apertures. Finally, the beam is projected onto the sample. The electron beam is scanned over a small area, and the secondary electrons, scattered electrons, and the characteristic X-rays are detected by electron detectors and an X-ray detector, respectively. A semiconductor detector is used for X-ray detection. This configuration is called the energy dispersive spectrometry (EDS). The merits of SEM-EDS are (i) the spectra for all elements are recorded in one scan, so measurement time is very short; (ii) secondary and backscattering electron images are better than that of an electron probe micro analyzer (EPMA) (see Figure 1.3), because the detector positions are designed to collect these electrons; and (iii) the price of SEM-EDS is on-third to one-fourth of that of EPMA. In case that the electron beam does not cover the whole sample, an $x-y$ stage is equipped to move the whole sample.

micro analysis (EPMA; see Figure 1.3) were developed. The geochemists today first observe, describe, and analyze using these techniques to retrieve as much as possible the phase and information on the major elements from samples.

1.1.1.1 X-ray Fluorescence Spectrometer

Details of the XRF spectrometer are shown in Figure 1.4. XRF is mainly applied for the analysis of solid samples. Generally, about 100 mg sample is diluted with 10 times a flux, which is composed of a mixture of pure $LiBO_2$ and $Li_2B_4O_7$, and melted into a glass bead in a Pt crucible. As the mass number increases, the absorption of X-rays also increases, and therefore lithium borate is ideal material to make the glass bead for measurement of the emitted X-rays.
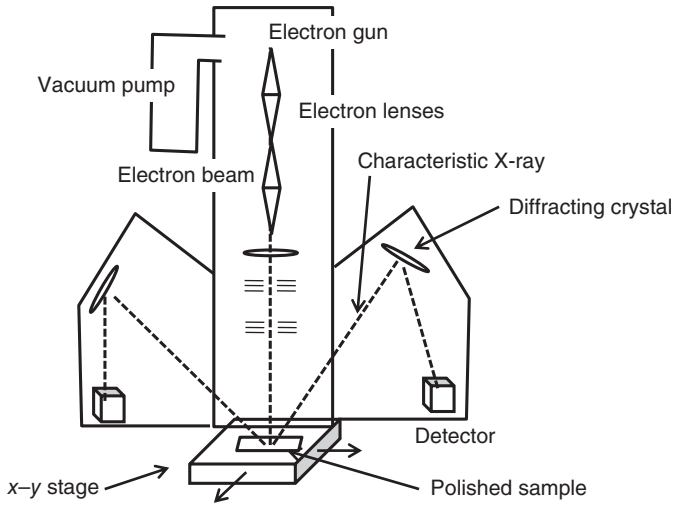
Figure 1.3 Schematic diagram of electron probe micro analyzer (EPMA). The electron gun, lenses, apertures are almost the same as those of SEM. The difference is in the collection and determination of characteristic X-rays. Characteristic X-rays emitted from the sample are diffracted by the crystals and collected by X-ray detectors. The position and material of the diffracting crystals are changed according to the wavelengths of characteristic X-rays of the target elements. This is called the wave length dispersive spectrometry (WDS). Five sets of diffracting crystals are maximally placed, and 10 elements can be determined in two scans. The merits of WDS are (i) the resolution of the characteristic X-ray is higher; therefore (ii) the background is lower; and (iii) X-ray diffraction is independent of the detector. Therefore, the diffracting crystal and the detector are chosen separately. Thus (iv) detection and diffraction correction are independent of the X-ray wavelength. Spot analysis of EPMA is simple. The polished and carbon-coated sample is set on the sample stage. The sample is bombarded by the electron beam, and the characteristic X-rays are measured. If more than five elements are to be measured, the diffraction crystals and their positions are changed, and the characteristic X-rays are measured again. The concentration is calculated by a so-called ZAF correction method using standard materials. Z, A, and F mean influences from the atomic number, X-ray absorption, and secondary fluorescence, respectively. The precision of elemental analysis is highly dependent on the standard materials. The stage is moved along the x and y directions on the x–y stage. The scanning (mapping) analysis is a feature of SEM-EDS and EPMA. The measurement time of each point is the X-ray integration time. Scanning measurement by WDS takes a very long time, and therefore only the spot analysis should be done by WDS. The size of the X-ray is 2.5 μm in diameter, and therefore a scanning stage of <2.5 μm is meaningless.

To minimize loss of the secondary X-rays, the chamber is kept under vacuum. Air is made of N_2 and O_2, and their mass numbers are higher than those of Li or B. Therefore, X-rays are absorbed or scattered by these gases. Vacuum is also sought to prevent deliquescence of the diffracting crystals.

(The author's monology: Modern XRF is fully automatic and sophisticated, so we sometimes forget that the XRF machine is a spectrometer. It is suggested that
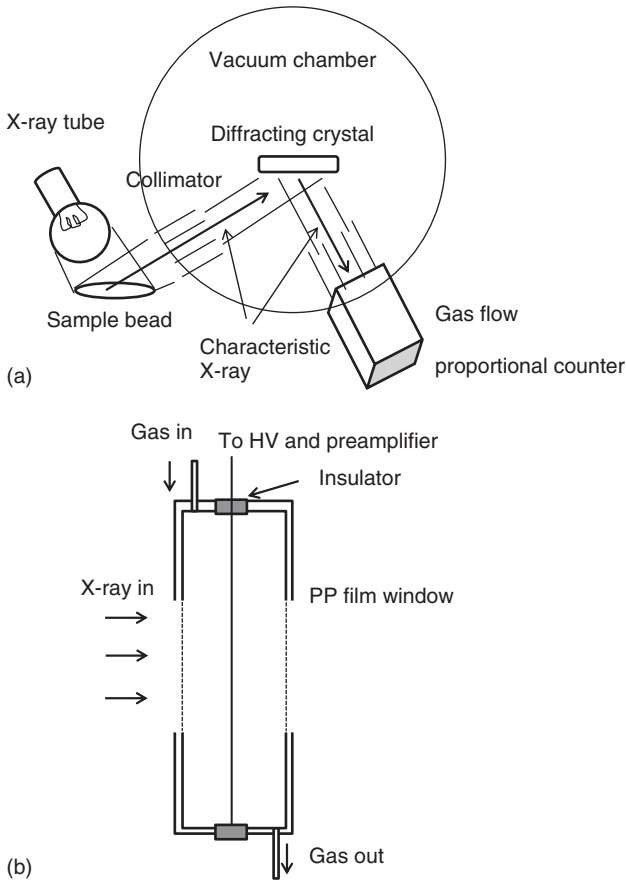
Figure 1.4 Schematic diagrams of (a) an X-ray fluorescence spectrometer and (b) a gas proportional counter. X-rays produced by the X-ray tube are made to fall on a sample bead. A Rh anode X-ray tube is often used. Secondary characteristic X-rays are emitted from the sample. X-rays are collimated onto the diffracting crystal by the primary collimator. From the entrance of the primary collimator to the detector, the chamber is kept in vacuum. Then the beams enter the diffracting crystal. There are various crystals suitable for the energy of X-rays, such as LiF, pentaerythritol crystal (PET), thallium acid phthalate crystal (TAP), and so on, and crystals can be exchanged easily without breaking the vacuum. The diffracted characteristic X-rays are measured by (b) a gas flow proportional counter, which counts the pulses. The counter is a metal box filled with a mixture of Ar and CH_4. There are two windows made of PP (polypropylene) film for X-ray input and output. There is a wire in the center to which a high voltage is supplied and the preamplifier is connected. When X-rays fall on the counter, they ionize the gas and electrons are generated and amplified. Thus an electric pulse is counted. In a modern XRF spectrometer, wavelengths of characteristic X-rays of each element are automatically chosen, characteristics of the counter are automatically compensated, and deconvolution of peak overlaps is automatically performed.

you see a spectrum (energy or wavelength vs counts per second) of one element like phosphorus at least once when you use an XRF spectrometer.)

1.1.1.2 Loss on Ignition and Ferric/Ferrous Ratio of Iron

For the determination of the major elements precisely, determinations of H_2O $(-)$, H_2O $(+)$, LOI (loss on ignition), and the ferric/ferrous ratio (Fe(II)/Fe(III)) are required. H_2O $(-)$ is weight of absorbed water. This is measured by the difference between the weight of the sample at room temperature and that after heating it at $105\,°C$. For hard silicate rock, this is negligible, but this becomes important for fresh deep-sea sediments.

LOI is weight difference between the raw sample and that heated at $1000\,°C$ in a porcelain crucible. This is easy to measure, so, in recent papers only LOIs are sometimes described. LOI is given by

$$LOI = H_2O(-) + H_2O(+) + \text{gaseous phases}\,(S, SO_4^{2-}, CO_3^{2-}, \text{etc.})$$
$$- \text{weight addition by FeO to Fe}_2O_3 \qquad (1.1)$$

where H_2O $(+)$ is the weight of water in structure. In XRF determination, the sample after the LOI measurement is used, and iron is calculated and obtained as Fe_2O_3, because all FeO is oxidized into Fe_2O_3 during making glass beads.

The amount of FeO or the ferric/ferrous ratio is obtained by a separate measurement of the sample [10, 11]. Briefly, the following reaction is used.

$$V(V) + Fe(II) \rightarrow V(IV) + Fe(III) \qquad (1.2)$$

The excess $V(V)$ is added and the sample is decomposed with $HF + H_2SO_4$. Then, the excess (unreacted) $V(V)$ is back-titrated with $Cr(VI)$. The method is robust, but uses non-green chemicals, which is a drawback of this method. Both $V(V)$ and $Cr(VI)$ are strongly toxic to the environment. The new method in which both $V(V)$ and $Cr(VI)$ are not used is required.

1.1.2
Trace Element Geochemistry

1.1.2.1 From REE Geochemistry to Trace Element Geochemistry

Modern geochemistry was started by Goldschmidt (1888–1947), who is called as Father of geochemistry. He categorized elements into lithophiles, chalcophiles, siderophiles, and atmophiles (see Figure 1.5). The lithophile elements reside in the silicate parts of earth such as the mantle and the continental crust. The chalcophile elements are preferentially combined with sulfur. The siderophile elements prefer metallic iron, and reside in the core. Although the boundary between siderophile and chalcophile is vague, this classification of elements is still used in modern analytical geochemistry.

Goldschmidt advocated that the distribution of elements into minerals is controlled by the ionic radius and valence. This idea is still correct, and based on this rule, the rare earth element (REE) geochemistry started.

H																	He
Li	Be											B	C	N	O	F	Ne
Na	Mg											Al	Si	P	S	Cl	Ar
K	Ca	Sc	Ti	V	Cr	Mn	Fe	Co	Ni	Cu	Zn	Ga	Ge	As	Se	Br	Kr
Rb	Sr	Y	Zr	Nb	Mo		Ru	Rh	Pd	Ag	Cd	In	Sn	Sb	Te	I	Xe
Cs	Ba	L	Hf	Ta	W	Re	Os	Ir	Pt	Au	Hg	Tl	Pb	Bi	Po	At	Rn
Fr	Ra	A	Rf	Db	Sg	Bh	Hs	Mt	Ds	Rg							

L		La	Ce	Pr	Nd		Sm	Eu	Gd	Tb	Dy	Ho	Er	Tm	Yb	Lu
A		Ac	Th	Pa	U	Np	Pu	Am	Cm	Bk	Cf	Es	Fm	Md	No	Lr

Li Lithophile   Fe Siderophile   Pb Chalcophile   Ar Atmophile

Figure 1.5 Geochemical categorization of elements by Goldschmidt.

The REE pattern consists of a plot in which the REE is placed in the order of the atomic number in the horizontal axis and the logarithms of the REE concentration normalized to the chondritic value in the vertical axis (see Figure 1.6; it was also called as a Masuda−Coryell diagram). The REE pattern uses the smooth decrease of ionic radii of REE as the atomic number increases. As all data in Figure 1.6 were obtained by isotope dilution-thermal ionization mass spectrometry (ID-TIMS), the mono-isotopic elements such as Pr, Tb, Ho, and Tm could not be determined. Details of ID (isotope dilution) and TIMS will be explained in Sections 1.1.2.2 and 4.5.1, respectively.

Together with the REE pattern, the ideas of distribution coefficients and the partial melting were introduced into REE geochemistry. We assume that the total system is partially melted. The weights of the liquid, the solids, and the total are M_L, M_S, and M, respectively. Those of REEs, T, are distributed based on the distribution coefficient K_d. The K_d value is defined as

$$K_d = C_S/C_L \tag{1.3}$$

where C_S and C_L are concentrations of the element T in solid and liquid forms, respectively. When the melt fraction F is introduced
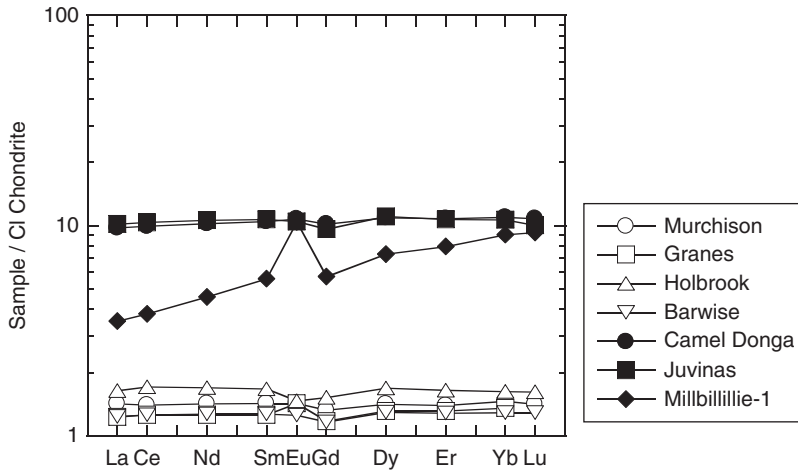
$$M_L = FM; \quad M_S = (1-F)M \tag{1.4}$$

$$m_L = fm; \quad m_S = (1-f)m \tag{1.5}$$

The weights of the element T in the liquid, solid, and total are m_L, m_S, and m, respectively. Then, Eqs. (1.3)−(1.5) become

$$K_d = C_S/C_L = (m_S/M_S)/(m_L/M_L) = (1-f) \times F/[f \times (1-F)]$$

or

$$F = fK_d/(1 + fK_d - f) \tag{1.6}$$

Figure 1.6 REE pattern of meteorites. Data are from Makishima and Masuda [12]. Murchison, Granes, Holbrook, Barwise are CM2, L6, L6, and H5 chondrites, respectively. Camel Donga, Juvinas, and Millbillillie-1 are eucrites. The vertical axis shows the normalized value to CI chondrite [13]. All data were obtained by isotope dilution-thermal ionization mass spectrometry (ID-TIMS).

This equation indicates that, if K_d is determined previously, and f is obtained from the sample, the fraction of partial melting, F, can be estimated.

As ID-TIMS was the only method to yield precise REE concentration data during 1960–1980s, and the REE pattern was the only sophisticated method to characterize the samples at that time, the cutting-edge studies in geochemistry were only for those who could analyze samples with ID-TIMS. However, REE measurement was not easy even for the bulk samples. Therefore, the REE geochemistry was used in or by a limited number of laboratories or scientists. Thus the REE geochemistry was in the golden era, and the famous books of Henderson [14] and Lipin and McKay [15] were published.

For the evaluation of the analytical methods, the detection limit is very important. The detection limit is generally defined as the 3σ detection limit. When the peak is larger than the 3σ of background, we judge the peak as significant (see Figure 1.7). The concentration that corresponds to the 3σ of background is defined as the "3σ detection limit" or simply the "detection limit" in this book.

There already existed elemental analytical methods such as colorimetry and flame atomic absorption spectrometry (FAAS). However, with these methods, REEs could not be measured because of their poor detection limits. Fassel [16] invented the inductively coupled plasma atomic emission spectrometry (ICP-AES; Figures 1.8 and 1.9), which began to be used in geochemistry. The detection limits of many elements were in the nanograms per milliliter levels (see Figure 1.10) and measurements of geochemically important elements such as REE became available. In addition, multi-element measurements became possible. However, for the REE determination, there were severe overlaps of the
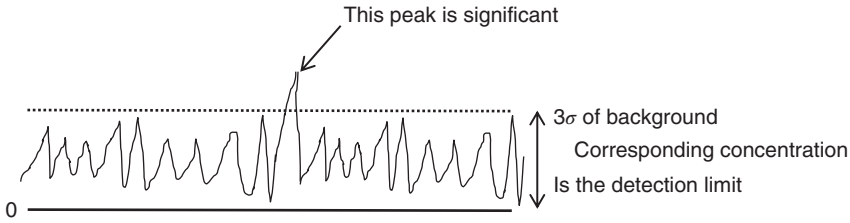
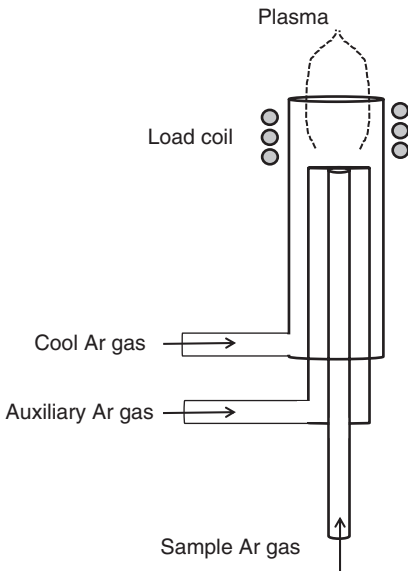**Figure 1.7** Definition of the 3σ detection limit.

Figure 1.8 Inductively coupled plasma torch. Ar gas as a cooling gas, as an auxiliary gas, and as a sample gas is supplied to the plasma torch. The innermost sample gas carries an aerosol of a sample solution. The load coil, through which cooling water is circulated, surrounds the apex of the torch and supplies energy to the inductively coupled plasma. The inductively coupled plasma is Ar plasma at atmospheric pressure, and therefore handling is easy.

photo-spectra between each REE, so that the accuracy was far lower than that of ID-TIMS by the overlap correction.

In TIMS, the detection limit is not very significant. This is because, when TIMS is used, sufficient amounts of a sample are decomposed to prepare required amounts of the target element ($\sim$10 ng). In addition, this amount is required for a signal of sufficient intensity to last for adequate data-acquisition time in order to obtain satisfactory precision.

At the beginning of 1980s, Houk *et al.* [17] and Date and Gray [18] invented the inductively coupled plasma Q-pole mass spectrometry (ICP-QMS; see Section 4.5.3 and Figure 4.29). The plasma in Figure 1.8 is $6000-10\,000\,\mathrm{K}$, and therefore it was a good source not only for the atomization but also for the ionization. Most elements including REEs are ionized to almost 100%. The detection limits of many elements became single-digit ppb levels (see Figure 1.11). When Figures 1.10 and 1.11 are compared, the detection limits seem to become worse in the case of ICP-QMS. However, mass spectrometry was simple and straightforward compared to photospectrometry like ICP-AES, and therefore the accuracy of
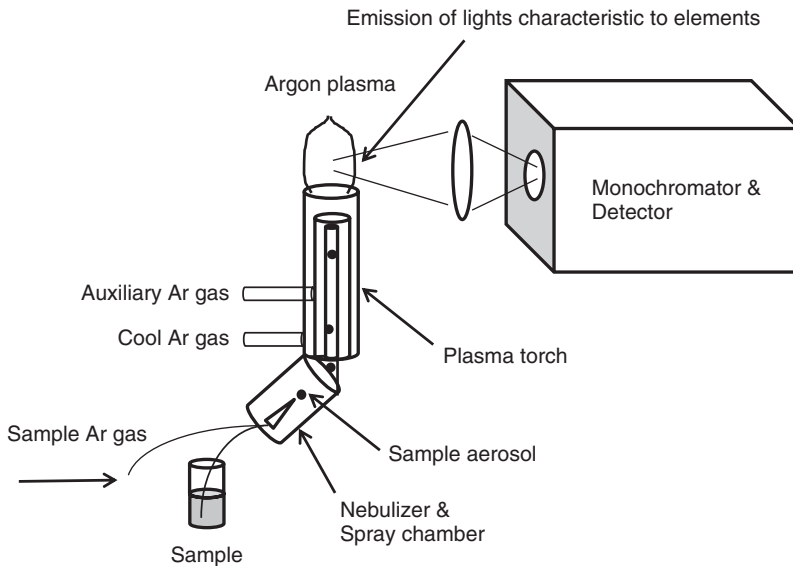
Figure 1.9 Schematic diagram of inductively coupled plasma atomic emission spectrometer (ICP-AES). The temperature of the plasma is so high that most elements are atomized or ionized and emit various wavelengths of lights characteristic of the elements. The emitted light is collected, diffracted by a monochromator, and detected. The number of available elements in ICP-AES is much larger than in an atomic absorption spectrometer. Especially, geochemically important rare earth elements (REEs), such as La, Ce, … , Yb, and Lu) can be measured by ICP-AES. Thus ICP-AES is used widely.
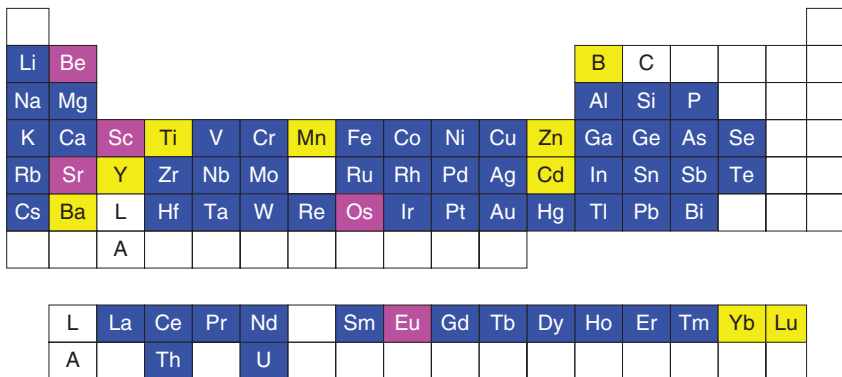
Figure 1.10 3σ detection limits of ICP-AES for each element. The data are after Ref. [1].

Li												B					
Na	Mg											Al	Si	P			
		Sc	Ti	V	Cr	Mn	Fe	Co	Ni	Cu	Zn		Ge	As	Se		
Rb	Sr	Y	Zr	Nb	Mo		Ru	Rh	Pd	Ag	Cd	In	Sn		Te		
Cs	Ba	L			W	Re	Os	Ir	Pt	Au	Hg	Tl	Pb	Bi			
		A															

	L	La	Ce	Pr	Nd		Sm	Eu	Gd	Tb	Dy	Ho	Er	Tm	Yb	
	A		Th		U											

P	>10		Lu	1–10		ng ml^{-1}

Figure 1.11 3σ detection limits of ICP-QMS for each element. The data are after Ref. [1].

measurement drastically increased. For example, when REEs are measured in ICP-AES, the major elements are needed to be removed. In addition, the separation of each REE is required. In contrast, REEs can be directly determined by just dilution of the sample solution in ICP-QMS.

The calibration curves that could not be used in TIMS can be employed in ICP-QMS. Thus ID was not required, and measurement of all REEs except Pm became possible. The advantage of mass spectrometry over photospectrometry such as ICP-AES is that the isotope ratios can be determined in the former. Therefore, ID can be applied in ICP-QMS when higher precision and accuracy in analytical results are required.

As the innovation in analytical methods occurred, lithophile element abundances in addition to those of the REEs became available. The REE pattern was expanded and evolved into the trace element pattern. Furthermore, the trace elements found their position one by one to make the normal mid-ocean ridge basalt pattern to be a smooth line. These orders of elements are determined partly empirically and partly by the K_d values in major rock-forming minerals.

This order was afterward named as incompatibility, and generally used for the horizontal order of the trace element pattern. The vertical axis is the trace element concentrations that are normalized by the primitive mantle values (PM-normalized trace element patterns; McDonough and Sun [13], see Figure 1.12). The smoothness of the trace element pattern comes from the smoothness of K_d (distribution coefficients) of the trace elements in the major rock-forming minerals.

The idea of the incompatibility, trace element patterns, and the distribution coefficients are used in modeling and simulation between melt-solid, magma-residue, iron melt-silicate melt, and so on. The trace element pattern has peculiar features. For example, if plagioclase was crystallized and lost from the magma,
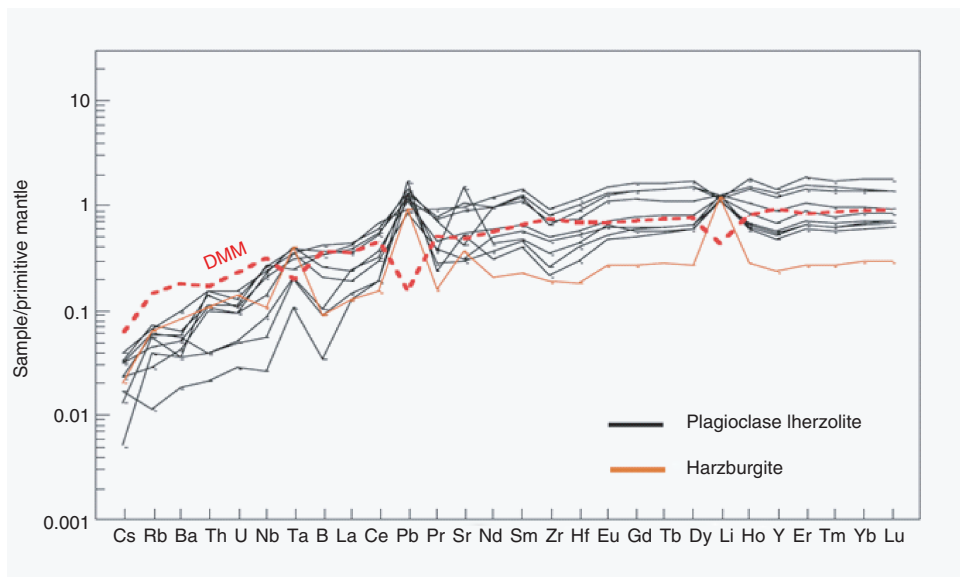
Figure 1.12 Example of the primitive mantle-normalized trace element patterns (PM-normalized trace element patterns) of the Horoman peridotite samples. Horoman is a peridotite massif located in the northern island, Hokkaido, Japan. The samples are plagioclase lherzolites and harzburgites. DMM means hypothetical Depleted MORB source Mantle. The plot is from Ref. [19] (Copyright Nature Publishing Group, authors permission from NPG, Ref. [19].)

Sr and Eu negative anomalies will appear in the pattern of the melt (magma). Because Sr and Eu have valence +2, they have higher distribution coefficients in plagioclase. If zircon was crystallized, Zr and Hf would show negative anomalies in the pattern. The alkaline elements, B, Pb, Sr, and Li should show peculiar behaviors if fluids or metasomatism-related materials affected the magma source. Thus the bulk trace element pattern is becoming the basic database of the silicate samples. It is like basic datasets such as blood pressure, various values of blood, hepatic, and urine tests of a patient who goes to a hospital.

1.1.2.2 Isotope Dilution Method (ID)

The ID method has already appeared several times from the beginning of this book. ID is necessary for elemental determination by TIMS because the signal intensity in TIMS is not proportional to the sample amount put into the TIMS machine. TIMS can give the precise isotopic ratio but the signal intensity itself cannot be used for the quantification of the element. In contrast, in ICP-QMS the signal is proportional to the element concentration. Therefore, the ID method is a prerequisite for quantitative analysis using TIMS.

Here, ID is explained using Figure 1.13. ID cannot be applied to mono-isotopic elements, such as Na, P, Co, Au, and so on. A target element needs to have two or more isotopes (1 and 2 in Figure 1.13). We obtain a "spike," which is artificially
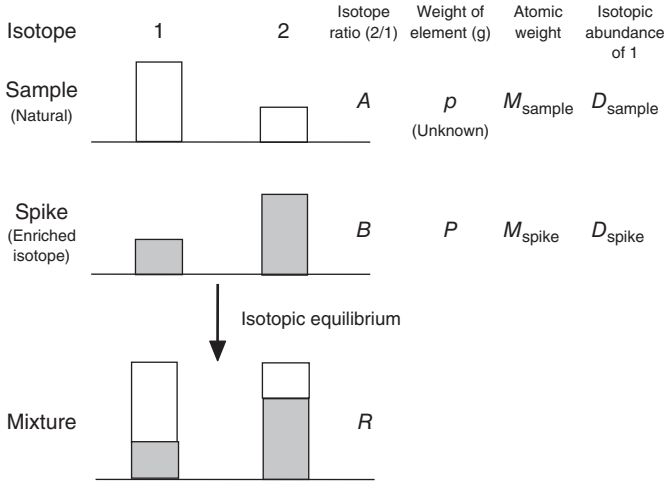
Figure 1.13 Conceptual diagram of isotope dilution.

enriched in one isotope. Here, 2 is the enriched isotope in the spike. Usually, the spike is prepared to be a solution. p and P are the weights (g) of the target elements in the sample and spike; A, B, and R are the isotope 2/isotope 1 ratios of the sample, the spike, and the sample–spike mixture; D_{sample} and D_{spike} are the isotopic abundances of isotope 1 in the sample and spike; and M_{sample} and M_{spike} are the atomic weights of the target element in the sample and spike, respectively.

The mole number of the mixture for the isotope 1 is

$$D_{sample} \times p/M_{sample} + D_{spike} \times P/M_{spike} \tag{1.7}$$

The mole number of the mixture for the isotope 2 is:

$$D_{sample} \times p/M_{sample} \times A + D_{spike} \times P/M_{spike} \times B \tag{1.8}$$

Thus the isotopic ratio of the mixture, R, is as given in Eq. (1.8)/Eq. (1.7):

$$R = \frac{D_{sample} \times p/M_{sample} \times A + D_{spike} \times P/M_{spike} \times B}{D_{sample} \times p/M_{sample} + D_{spike} \times P/M_{spike}} \tag{1.9}$$

The amounts of the target element in the sample are calculated by the following equation by transforming Eq. (1.9) into Eq. (1.10).

$$p = \frac{B - R}{R - A} \times \frac{D_{spike}}{D_{sample}} \times \frac{M_{sample}}{M_{spike}} \times P \tag{1.10}$$

Equation 1.10 can be rewritten as

$$p = C_T^{sample} \times m_{sample} = \frac{B - R}{R - A} \times Q \times P$$

$$C_T^{sample} = \frac{B - R}{R - A} \times Q \times C_{spike} \times m_{spike}/m_{sample}$$

$$Q = \frac{D_{spike}}{D_{sample}} \times \frac{M_{sample}}{M_{spike}} \tag{1.11}$$

$$C_T^{\text{sample}} = \frac{B-R}{R-A} \times Q' \times m_{\text{spike}}/m_{\text{sample}}$$

$$Q' = \frac{D_{\text{spike}}}{D_{\text{sample}}} \times \frac{M_{\text{sample}}}{M_{\text{spike}}} \times C_{\text{spike}} \tag{1.12}$$

where C_T^{sample} and C_{spike} are the concentrations of the target element in the sample and spike; m_{sample} and m_{spike} are the sample and spike weights; p and P are the net sample and spike weights; and Q' in Eq. (1.12) is the pseudo-concentration of the spike because it has the dimension of concentration. The pseudo-concentration of the spike solution is calibrated by measurements of several mixtures of the spike and the standard solutions using TIMS or ICP-QMS.

The merit of introducing Q' is that there is no need to determine D_{spike}, which is the atomic abundance of the spike. For the atomic abundance calculation, all isotopes need to be measured. However, when a small interference exists on some isotopes of the target element, D_{spike} cannot be determined precisely. However, when Q' is used, the ID equation (1.12) can be applied by only making mixtures of the spike and sample and measuring isotope ratio (isotope 2/isotope 1).

If A, B, and Q' are determined previously, and m_{sample} and m_{spike} are measured for each sample, the concentration of the target element is determined by only measuring R from Eq. (1.12). This equation stands as long as the isotope equilibrium for the target element is achieved. The largest merit of ID is that, once isotope equilibrium is achieved, losses of the target element by the ion exchange column chemistry or solvent extraction, or by poor handling, do not affect the determination of the result.

The precision of the spike concentration affects directly the precision of the measurement. In addition, isotope ratios of natural and spike abundance also affects the accuracy of the measurement. Therefore, the most accurate analytical method such as TIMS is recommended for the calibration of these basic parameters even when ICP-QMS is used for ID. The isotopic abundances of the spike are provided in the analytical sheet issued by the company, but it is only for reference and the isotope ratios must be determined by yourself.

1.1.2.3 Error Magnification

Here we investigate how the error in the determination of R is propagated to the concentration result (the error magnification or error propagation) in ID. To make the equation simpler, $Q'' = Q' \times m_{\text{sample}}/m_{\text{spike}}$ is applied, and derivative of Eq. (1.12) for R becomes

$$dC_T^{\text{sample}}/dR = Q'' \times \frac{A-B}{(A-R)^2} \tag{1.13}$$

From Eq. (1.12)

$$\frac{dC_T^{\text{sample}}}{C_T^{\text{sample}}} = R \times (B-A)/[(A-R) \times (B-R)] \times dR/R \tag{1.14}$$

$$= F(R) \times dR/R \tag{1.15}$$
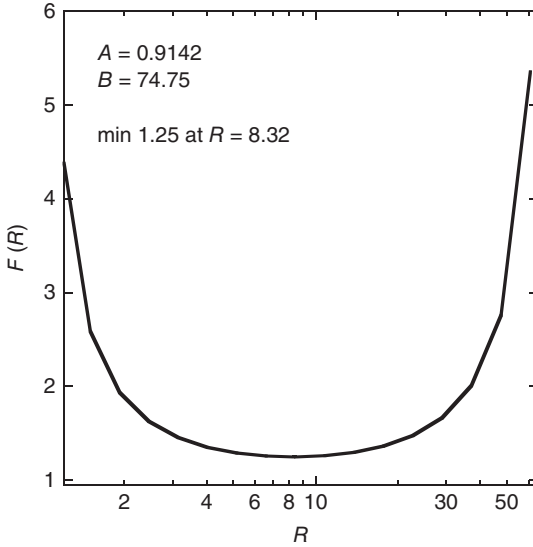
Figure 1.14 Error magnification. This function takes a minimum value of 1.25 at $R = 8.32$.

where

$$F(R) = R \times (B - A)/[(A - R) \times (B - R)] \qquad (1.16)$$

$F(R)$ is a function that indicates that the deviation of R (dR/R) is magnified to the deviation of the concentration ($dC_T^{\text{sample}}/C_T^{\text{sample}}$).

If we take the derivative of $F(R)$, we get

$$dF(R)/dR = (B - A) \times (R^2 - A \times B)/ [(R - B) \times (A - R)^2] \qquad (1.17)$$

This function becomes a minimum when $dF(R)/dR = 0$ at $R = (A \cdot B)^{0.5}$.

For example, if we plot $F(R)$ against R when $A = 0.9142$, $B = 74.75$ (a case of Sm; ^{149}Sm/^{147}Sm), the result is as shown in Figure 1.14. According to the figure, the function $F(R)$ takes a minimum value of 1.25 at $R = 8.32$. $F(R)$ means, for example, when the measurement error is 0.1%, the minimum error using ID is 0.125% (1.25×0.1%). If R is smaller or larger than 8.32, the error in ID is magnified by $F(R)$. When you want 0.2% error after ID, R should be between ~2 and ~40. If R is outside this range (underspiked or overspiked), the error in ID is >0.2%, and therefore the data should be discarded.

1.1.2.4 Isotope Dilution with Internal Standardization Method (ID-IS)

If the intensity ratios for element J over the isotope 1 of the target element T is proportional to the concentration of element J, in other words, isotope 1 can be used as the internal standard, an isotope dilution with internal standardization method (ID-IS) can be applied [20–23].

We prepare a multielement standard solution, which contains the target element J. The target element can be plural. We also prepare the sample solution that is already spiked for the element T. Intensity ratios for each isotope of the element J over the isotope 1 of the target element of the sample and the standard solution are defined as

$$S_J^{\text{sample}} = \frac{I_J^{\text{sample}}}{I_T} \tag{1.18}$$

and

$$S_J^{\text{std}} = \frac{I_J^{\text{std}}}{I_T} \tag{1.19}$$

where I is the intensity. Note that no spike is added in the standard solution.

The author suggests the use of the GSJ (Geological Survey of Japan) standard material, JB-3, as the internal standard material, because it is still available (in 2014). The elemental or isotopic ratios of JB-3 sometimes appear through this book. The recommended concentrations of the elements by the author are summarized in Table 1.2.

The relative concentration factor (f_J) for the element J against isotope-1 of the element T, which is the ratio of the concentration in the solution per the signal intensity of the measured isotope, is defined as

$$f_J = \frac{X_J^{\text{std}}/I_J^{\text{std}}}{X_T^{\text{std}}/I_T^{\text{std}}} = \frac{X_J^{\text{std}}/X_T^{\text{std}}}{S_J^{\text{std}}} \tag{1.20}$$

where X_J^{std} and X_T^{std} are the concentrations of the element J and T in the standard solution. The concentration of the element J in the sample (X_J^{sample}) is obtained from measurement of the sample solution as

$$X_J^{\text{sample}} = X_T^{\text{sample}} \cdot f_J \cdot I_J^{\text{sample}}/I_{T*}^{\text{sample}} \tag{1.21}$$

where I_J^{sample} is the intensity of the element J in the sample solution and I_{T*}^{sample} is the net intensity of isotope 1 from the sample without a spike contribution. In ID, I_{T*}^{sample} is obtained as

$$I_{T*}^{\text{sample}} = I_T^{\text{sample}} \cdot (B - R)/(B - A) \cdot A/R \tag{1.22}$$

From Eqs. (1.20) to (1.22), we obtain

$$X_J^{\text{sample}} = X_T^{\text{sample}} \cdot (B - A)/[(B - R) \cdot A] \cdot R \cdot f_J \cdot S_J^{\text{sample}} \tag{1.23}$$

To apply the ID-IS method, the relative concentration factor (f_J) needs to be constant. This can be achieved by ICP-QMS, because in this method the ionization efficiencies of all elements are ~100%. However, in TIMS, a single element is loaded on the filament, and therefore it cannot be applied in most cases.

Table 1.2 Recommended elemental concentrations in JB-3 for the ID-IS method.

Makishima and Nakamura [20]			Lu *et al.* [23]	
(μg g^{-1})		(μg g^{-1})		(μg g^{-1})
Li	7.28	Sc	34.2	B	20.7
Be	0.628	V	384	Zr	86.2
Rb	14.0	Co	35.1	Nb	1.87
Sr	414	Ni	37.0	Mo	1.12
Y	23.1	Cu	179	Sn	1.04
Cs	0.928	Zn	114	Sb	0.104
Ba	239	Ga	20.7	Hf	2.65
La	8.12			Ta	0.114
Ce	20.9		(%)		(%)
Pr	3.14	Al$_2$O$_3$	17.5	TiO$_2$	1.37
Nd	15.9	Fe$_2$O$_3$^{T}	12.0		
Sm	4.17	MnO	0.184		
Eu	1.31	MgO	5.19		
Gd	4.77	CaO	9.7	Wang *et al.* [24]	
Tb	0.741	Na$_2$O	2.74		(μg g^{-1})
Dy	4.66	K$_2$O	0.790	F	261
Ho	0.949	P$_2$O$_5$	0.294	Cl	292
Er	2.69				
Tm	0.380	Makishima *et al.* [22]			
Yb	2.50		(μg g^{-1})		
Lu	0.377	Cd	0.111		
Pb	4.85	In	0.069		
Th	1.30	Tl	0.047		
U	0.480	Bi	0.031		

Makishima and Nakamura [25]

	(μg g^{-1})
S	5.64

Makishima and Nakamura [21]

	(μg g^{-1})
Ge	1.23
As	1.43
Se	0.057
Te	0.0010

1.1.3
Determination of Mass Fractionation

We have other strong weapons in analytical geochemistry: stable isotopes. As soon as isotopes were discovered, isotopic fractions were observed in H, O, C, N, S, and so on. For this purpose, the stable isotope mass spectrometer or the isotope ratio mass spectrometer (IRMS) has been developed. Such mass spectrometry is

beyond the scope of this book. Briefly, the target element is separated using gas lines and ionized by electron bombardment. The target element ions are separated by a sector magnet and detected in similar way as in TIMS.

The determination of isotopic fractionation of metallic elements such as Li, Mg, Ca, Fe, and so on, was sometimes tried by TIMS, but only a small number of elements were successful, because thermal ionization occurs only in a limited number of elements and the condition of loaded samples on the filaments was reproducible.

There are similar terms, "mass fractionation" and "mass discrimination." In this book, the mass fractionation indicates "mass-dependent mass fractionation that occurs in nature," and mass discrimination is "mass-dependent phenomena that occur in the mass spectrometer or under artificial conditions such as evaporation or ion exchange column chemistry in sample preparation."

Here, mass fractionation is explained in more detail. When there are two isotopes of the target element T, and the isotope ratio is R, the mass fractionation is usually expressed as

$$\delta T\,(\text{‰}) = (R_{\text{sample}}/R_{\text{standard}} - 1) \times 1000 \tag{1.24}$$

where R_{sample} and R_{standard} indicate the isotope ratios of the sample and standard, respectively. Generally, when the isotope ratio R is defined, the heavier and the lighter isotope become the numerator and denominator, respectively.

If there are more than three isotopes in one element, the mass fractionation occurs following mass fractionation laws. We choose two of the three isotopes for the reference isotope ratio. Then, the mass fractionation of the third isotope, which is not used in the reference isotope, could follow the mass fractionation law as described below.

Here we assume that u, v, and r are the denominator, target, and reference isotopes; R_{m} is the observed target isotope ratio v/u; R_{c} is a constant ratio without the mass fractionation ratio v/u; R_{r} is a constant reference isotope ratio r/u; R_{rm} is the observed reference isotope ratio (r/u); and α is a mass fractionation factor per mass. Then, the isotope ratios follow the mass fractionation law (the linear law), which is written as

$$R_{\text{m}} = R_{\text{c}} \times [1 + \alpha x(v - u)] \tag{1.25}$$

$$\alpha = \frac{R_{\text{rm}}/R_{\text{r}} - 1}{r - u} \tag{1.26}$$

The Rayleigh fractionation is as follows:

$$R_{\text{m}} = R_{\text{c}} \times [1 + \alpha]^{[1 - \sqrt{(u/v)}]/[1 - \sqrt{(u/r)}]} \tag{1.27}$$

$$\alpha = \left[\frac{\sqrt{(u/v)}}{\sqrt{(u/r)}} \right] \times \left(\frac{R_{\text{rm}}}{R_{\text{r}}} \right) - 1 \tag{1.28}$$

Similar equations appear in the mass discrimination correction (Section 5.2.2).

Figure 1.15 Biochemically important elements. "Essential" means essential elements to life. "Toxic" is toxic elements to life. "Useful (drugs, etc.)" indicates useful elements used in drugs, therapies, and so on. The data is mainly based on Crichton [26]. Lithium has psychopharmacological effects. Titanium is used for supporting fractured bones. Radioactive Ga isotope is used for tumor analysis of the whole human body. Zirconium, Pd, Ag, Pt, and Au are used in dental therapy. Barium and Gd are used for X-ray and magnetic resonance imagings (MRIs), respectively. Radium is contained in some hot springs.

After the invention of multicollector-inductively coupled plasma-mass spectrometry (MC-ICP-MS, which is always compared with TIMS), natural isotopic fractionation of metallic elements such as Fe, Cu, Zn, Mo, Cd, Tl, and so on, has been extensively studied by large number of researchers, because these elements are expected to be biologically important and detectable fractionation is expected to occur. Furthermore, the standard-sample-bracketing (SSB) method or a simultaneous mass discrimination correction by other elements added to the target element in MC-ICP-MS increased the precision of the isotopic measurement and the number of available elements. These techniques expanded analytical geochemistry into bio-geochemistry. Biochemically important elements are shown in Figure 1.15, and many of them show mass fractionation.

1.1.4
Age Dating

The fourth strategy of analytical geochemistry is age dating. The naturally existing radioactive isotopes are shown in Table 1.3. The change of isotopic ratios by the radioactive decay can be used for age dating. In order to detect such isotopic ratio change of the daughter isotope or the radiogenic isotope, a mass spectrometer with higher precision is preferred. Magnetic-sector type mass spectrometers have the advantage over Q-pole type mass spectrometers because the precision of

Table 1.3 Radioactive isotopes and decay constants.

| Radioactive isotope	Decay scheme	Daughter isotope	Decay constant (yr^{-1})
^{40}K	EC	^{40}Ar	5.81×10^{-11}
	β^-	^{40}Ca	4.962×10^{-10}
^{87}Rb	β^-	^{87}Sr	1.42×10^{-11}
^{138}La	EC	^{138}Ba	4.44×10^{-12}
	β^-	^{138}Ce	2.29×10^{-12}
^{147}Sm	α	^{143}Nd	6.54×10^{-12}
^{176}Lu	β^-	^{176}Hf	1.867×10^{-11}
^{187}Re	β^-	^{187}Os	1.666×10^{-11}
^{190}Pt	β^-	^{190}Os	1.477×10^{-12}
^{228}Ra	Decay chain		0.12
^{232}Th	Decay chain	^{228}Ra	4.9475×10^{-11}
^{231}Pa	Decay chain		2.116×10^{-5}
^{235}U	Decay chain	^{231}Pa	9.8485×10^{-10}
^{226}Ra	Decay chain		4.28×10^{-4}
^{230}Th	Decay chain	^{226}Ra	9.1577×10^{-6}
^{234}U	Decay chain	^{230}Th	2.826×10^{-6}
^{238}U	Decay chain	^{234}U	1.55125×10^{-10}

Decay constants are from Dickin [27].

the former is far better. For example, 0.01% can be achieved by a magnetic-sector type mass spectrometer like TIMS, while 0.3% is the best precision by ICP-QMS. The higher precision in mass spectrometry can enable the detection of smaller radiogenic variation of isotopic ratios by the radioactive decay, resulting in higher resolution for age dating of geological events.

1.1.4.1 Types of Radioactive Decay

There are six main radioactive decay types of radioactive isotopes: α-decay, β^--decay, double β^--decay, β^+-decay, electron capture (EC), and spontaneous fission (SF). α-Decay is where an α-particle is emitted. There is a decrease of two protons and two neutrons, and the mass number decreases by four. β^--Decay corresponds to electron emission. Therefore, the proton number increases by one with the same mass number. A double β^--decay occurs when a single β^--decay nucleus has higher energy or is forbidden. The β^+-decay is a positron emission. Therefore, the proton number decreases by one with a constant mass number. EC occurs when an electron is absorbed in the nucleus. Therefore, the proton number decreases by one with a constant mass number. SF occurs when the nucleus decays into two nuclei. This occurs only in heavy nuclei such as ^{235}U, ^{238}U, and ^{240}Pu.

The change in the N (neutron number) versus Z (proton number) plot is summarized in Figure 1.16a, and the fission yield of ^{235}U is shown in Figure 1.16b. The curve shows the two maxima of the fission yield $\sim 85 - 105$ (Sr, Y, Zr, Nb, Mo, Tc, and Ru) and $\sim 135 - 155$ (Xe, Cs, Ba, La, Ce, Pr, Nd, Pm, Sm, Eu, and Gd).

(a)

(b)
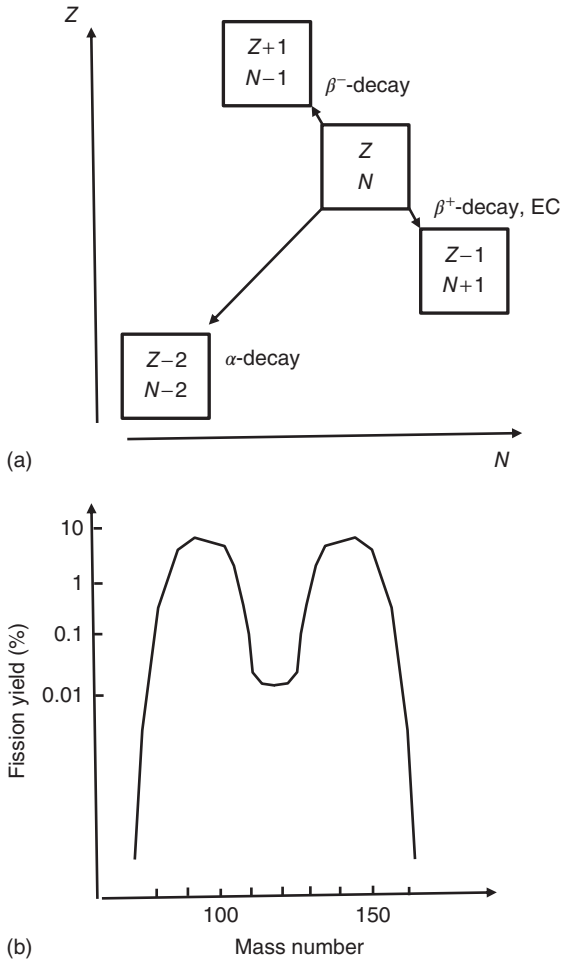
Figure 1.16 Radioactive decays. (a) The changes of N (neutron number) and Z (proton number) by the radioactive decays. (b) Possibility of spontaneous fission yield of ^{235}U. Note that the vertical axis is logarithmic.

1.1.4.2 Age Dating by Radioactive Isotopes

Radioactive decay is expressed by the following equation, when N is the number of radioactive isotopes:

$$\frac{dN}{dt} = -\lambda N \tag{1.29}$$

λ is called as the *decay constant*. The half-life, $T_{1/2}$, is related to λ as

$$T_{1/2} = \ln 2/\lambda = 0.693/\lambda \tag{1.30}$$

When Eq. (1.29) is integrated, we get

$$N_t = N_0 e^{-\lambda t} \tag{1.31}$$

N_0 is the initial number of the radioactive isotope and t is the elapsed time from the start. The number of the daughter isotope is

$$D_t = D_0 + (N_0 - N_t) = D_0 + N_0(1 - e^{-\lambda t}) \tag{1.32}$$

However, in geochemistry, $T = 0$ and T is the age of the sample. In this case, $N_0 = N_P e^{\lambda T}$ from Eq. (1.32), and $D_t = D_P$, where the suffix "P" indicates "present." Thus Eq. (1.32) changes to

$$D_P = D_0 + N_0(1 - e^{-\lambda T}) = D_0 + N_P(e^{\lambda T} - 1) \tag{1.33}$$

For example, we consider the decay of ^{87}Rb to ^{87}Sr. From Eq. (1.32), we obtain the following equation where ^{87}Rb$_P$ is the "present" amount of Rb and T is the age of this isotopic system:

$$^{87}\text{Sr}_P = {}^{87}\text{Sr}_0 + {}^{87}\text{Rb}_P(e^{\lambda T} - 1) \tag{1.34}$$

Strontium has a stable isotope, ^{86}Sr, whose number does not change over the time T. Then $(^{86}\text{Sr})_P = (^{86}\text{Sr})_0$:

$$\left(\frac{^{87}\text{Sr}}{^{86}\text{Sr}}\right)_P = \left(\frac{^{87}\text{Sr}}{^{86}\text{Sr}}\right)_0 + \left(\frac{^{87}\text{Rb}}{^{86}\text{Sr}}\right)_P (e^{\lambda T} - 1) \tag{1.35}$$

This equation is the basic equation of age dating. In other words, the strontium isotope ratio at age T can be calculated by Eq. (1.35).

In actual applications, we use the isochron plot (see Figure 1.17). We measure $(^{87}\text{Sr}/^{86}\text{Sr})_P$ and $(^{87}\text{Rb}/^{86}\text{Sr})_P$ of several phases. If all the phases became isotopic equilibria at age T, and did not suffer any disturbances from T to present, the data should form a line, which is called an isochron as shown in Figure 1.17. If we calculate the y-intercept, it is the initial value of $(^{87}\text{Sr}/^{86}\text{Sr})_0$. The slope corresponds to the age. If the age becomes older and older, the slope becomes steeper and steeper. When we calculate a regression line including x and y errors, we use the calculation method developed by York [28]. This calculation is included in the famous ISOPLOT by the Berkeley Geochronology Center, which can be obtained free from their web site.
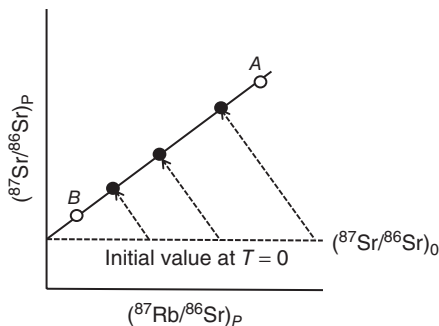

Figure 1.17 Isochron plot.

In order to obtain the age of magma formation, for example, the minerals must have been isotopically homogenized (the initial value must be the same). Second, the parent–daughter isotopic pair must have been in the closed system. If the system became open by metamorphism or alteration, the isochron method cannot be applied properly.

In addition, in order to obtain precise and accurate age data, both the isotope ratio $(^{87}Sr/^{86}Sr)_P$ and the parent–daughter isotope ratio $(^{87}Rb/^{86}Sr)_P$ must be determined as precisely as possible. Therefore, the measurement of the isotope ratio $(^{87}Sr/^{86}Sr)_P$ is done by TIMS. In addition, concentration determination of Rb and Sr is also performed by ID-TIMS because this method can give a precision of <0.3% for the Rb/Sr ratio, which cannot be achieved by other analytical methods.

Recently, MC-ICP-MS has developed very much and isotopic ratios seem to be measured a similar manner as in TIMS. However, there is an advantage in TIMS, where the purified element from the sample is loaded and heated on a filament (see Figure 4.11). The preferred temperature for evaporation and ionization differs from element to element. For example, Sr is ionized at a higher temperature than Rb. Therefore, the final separation of ^{87}Sr from ^{87}Rb can be performed on the filament in the mass spectrometer. In contrast, ICP (inductively coupled plasma) machines ionize every element with ~100% efficiency at the same time. There is no difference in ^{87}Sr and ^{87}Rb. This difference in ionization is very critical in very precise measurement of ^{87}Sr.

To use minerals that have a large parent–daughter ratio is very effective in the age dating. For example, in the Rb–Sr system, micas have very high Rb/Sr values. In contrast, plagioclase has a very low Rb/Sr ratio, which is almost the same as the initial value. In the case of Sm–Nd system, garnet has a high Sm/Nd ratio.

1.1.4.3 Extinct Nuclides

There are some nuclides that have relatively short half-lives of 0.1–100 Myr. These nuclides are extinct now. However, their existence can be found in the materials formed in the early solar system. Such nuclides are shown in Table 1.4. The half-lives of these elements are so short that they have already become extinct. Therefore, these elements are called *extinct nuclides*.

The existence of these elements in the early solar system has been proved in the fossil isochron, as shown in Figure 1.18. The differences from the isochron in Figure 1.17 are as follows: We use ^{26}Al for the example. As ^{26}Al is already extinct, we cannot use ^{26}Al in the horizontal axis in the isochron. The daughter isotope is ^{26}Mg, and Mg has nonradiogenic isotopes ^{24}Mg and ^{25}Mg. Thus the horizontal axis can be Al/Mg or $^{27}Al/^{24}Mg$ ($^{27}Al/^{25}Mg$ can be also used.). From the slope, the initial value of $^{26}Al/^{27}Al$ of 5×10^{-5} is obtained. To obtain this plot, very precise measurement of vertical axis, that is, $^{26}Mg/^{24}Mg$, is required. In addition, a very large value of Al/Mg is required. Actually, this plot is observed from plagioclase, which has a very high Al/Mg ratio. In olivine, the measurement of Mg isotope is very easy because Mg is contained in 10% levels; but the Al concentration in

Table 1.4 Some important extinct nuclides.

Radioactive parent	Decay scheme	Daughter isotope	Horizontal isotope ratio	Decay constant (yr^{-1})	Half life (Myr)
^{26}Al	β^-	^{26}Mg	^{27}Al/^{24}Mg	9.8×10^{-7}	0.7
^{60}Fe	$2\beta^-$	^{60}Ni	^{56}Fe/^{58}Ni	4.7×10^{-7}	1.5
^{53}Mn	β^-	^{53}Cr	^{55}Mn/^{52}Cr	1.9×10^{-7}	3.7
^{107}Pd	β^-	^{107}Ag	^{108}Pd/^{109}Ag	1.1×10^{-7}	6.5
^{182}Hf	$2\beta^-$	^{182}W	^{180}Hf/^{184}W	7.7×10^{-8}	9.0
^{129}I	β^-	^{129}Xe	^{127}I/^{132}Xe	4.3×10^{-8}	16
^{146}Sm	α	^{142}Nd	^{149}Sm/^{144}Nd	6.7×10^{-9}	103

The horizontal isotope ratio means the horizontal axis in the fossil isochron.
Decay constants are from Dickin [27].
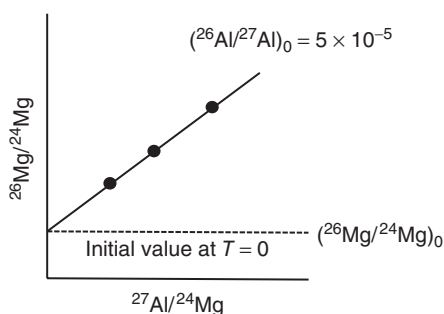
Figure 1.18 Fossil isochron plot.

olivine is too low to detect the variation. Thus choice of the appropriate mineral phase is very important.

In the Fe−Ni system, high Fe and low Ni phase, such as troilite, is a good target. In the Mn−Cr system, chromite is preferred as the origin. In the Pd−Ag system, iron meteorites are a target. In the Hf−W system, Hf is a lithophile and W is a siderophile, and the half-life is 9 Myr; therefore, the metallic core formation in the Earth, the Moon, and Mars can be discussed. In the Sm−Nd system, the half-life is 103 Myr, and therefore early differentiation of the Earth can be discussed.

1.1.4.4 An Isochron or a Mixing Line?

If there are independent components *A* and *B*, as shown in Figure 1.17, and they are mixed at present, they form a mixing line, which seems the same as the isochron discussed in Section 1.1.4.2. This is a simple mixing line, and sometimes ironically called an *errorchron*. In order to discriminate the isochron from the mixing line, there is a so-called 1/C test. The mixing line is expressed as

$$R_M = XR_A + (1 - X)R_B \tag{1.36}$$

where R_M, R_A, and R_B are isotope ratios of the mixed point and the points A and B, respectively. For the concentration

$$\frac{T_M}{S_M} = X\left(\frac{T_A}{S_A}\right) + (1 - X)\left(\frac{T_B}{S_B}\right) \tag{1.37}$$

where T_M, T_A, and T_B are concentrations of the radioactive element T (Rb) of the mixed point and the points A and B, respectively, S_M, S_A, and S_B are concentrations of the stable isotope of the radiogenic isotope S (^{86}Sr) of the mixed point and the points A and B, respectively.

Then Eq. (1.37) is re-formed into

$$1/S_M = X(T_A/S_A)/T_M + (1 - X)(T_B/S_B)/T_M \tag{1.38}$$

If α and β are defined as

$$\alpha = (T_A/S_A)/T_M; \quad \beta = (T_B/S_B)/T_M \tag{1.39}$$

then Eq. (1.38) can be written as

$$\frac{1}{S_M} = X\alpha + (1 - X)\beta \tag{1.40}$$

Then Eq. (1.40) is transformed into

$$X = (1/S_M - \beta)/(\alpha - \beta); \ 1 - X = (\alpha - 1/S_M)/(\alpha - \beta) \tag{1.41}$$

Using X and $1 - X$, Eq. (1.36) is rewritten as:

$$\begin{aligned} R_M &= R_A(1/S_M - \beta)/(\alpha - \beta) + R_B(\alpha - 1/S_M)/(\alpha - \beta) \\ &= (1/S_M)(R_A - R_B)/(\alpha - \beta) + (R_A\beta - R_B\alpha)/(\alpha - \beta) \end{aligned} \tag{1.42}$$

Therefore, when the isotope ratios are plotted against $1/S_M$ (i.e., inverse of concentration), the plot forms the line of Eq. (1.42). This easy but essential test is called as the 1/C test, and we can find that the isochron is actually the isochron or the mixing line. This test should be done in all cases when the isochron type data are obtained.

1.1.4.5 A Single Zircon Dating

Zircon is $ZrSiO_4$ and a common mineral in acidic rocks. This mineral is very refractory and stands against metamorphism, erosion, and weathering. The zircon crystal contains a high concentration of U but very low Pb in its structure; therefore, Pb in zircon is considered to be only radiogenic Pb. In this dating, two decays of uranium isotopes

$$^{238}U \rightarrow {}^{206}Pb^* \tag{1.43}$$

$$\left(\frac{^{206}Pb^*}{^{204}Pb}\right) = \left(\frac{^{238}U}{^{204}Pb}\right) \times (e^{T\lambda 8} - 1) \tag{1.44}$$

$$^{235}U \rightarrow {}^{207}Pb^* \tag{1.45}$$

$$\left(\frac{^{207}\text{Pb}^*}{^{204}\text{Pb}}\right) = \left(\frac{^{235}\text{U}}{^{204}\text{Pb}}\right) \times (e^{T\lambda5} - 1) \tag{1.46}$$

are used. The asterisks mean the radiogenic lead; T is crystallized age of the zircon, and $\lambda8$ and $\lambda5$ are the decay constants of ^{238}U and ^{235}U, respectively. The difference of Eqs. (1.44) and (1.46) from Eqs. (1.33) and (1.35) is that there are no initial terms in the former.

In addition

$$^{232}\text{Th} \rightarrow {}^{208}\text{Pb}^* \tag{1.47}$$

is used to evaluate the effect of common lead. "Common lead" means the initial lead incorporated in zircon. From Eqs. (1.44)–(1.46), we have

$$\left(\frac{^{206}\text{Pb}^*}{^{207}\text{Pb}^*}\right) = \left(\frac{^{238}\text{U}}{^{235}\text{U}}\right) \times (e^{T\lambda8} - 1)/(e^{T\lambda5} - 1) \tag{1.48}$$

$(^{238}\text{U}/^{235}\text{U})$ is constant and 137.88. Thus if $(^{206}\text{Pb}^*/^{207}\text{Pb}^*)$ is measured, T can be obtained. This is called the Pb–Pb dating method. In order to determine T precisely, accurate determination of the isotope ratio $^{206}\text{Pb}^*/^{207}\text{Pb}^*$ and selection of zircons without common lead are prerequisites. In addition, the choice if less disturbed zircons after formation is also important. "Disturb" means Pb or U is lost or added from outside of the zircon by geological processes such as metamorphism or weathering.

If $(^{206}\text{Pb}^*/^{238}\text{U})$ is plotted against $(^{207}\text{Pb}^*/^{235}\text{U})$, a curve that starts from the origin is obtained. This is called a concordia curve, which is shown in Figure 1.19. This is a combination of two U–Pb dating methods. If the data lie on this curve, the U–Pb of zircon has not been disturbed from formation of zircon to the present. If the data do not lie on this line, the U–Pb of zircon has been disturbed. If the disturbance was only once, the data form a line. One end shows the disturbing age (1 Ga in Figure 1.19), and the other end shows the formation age (3.5 Ga in Figure 1.19). This line is called a discordia line. This dating method is called the concordia method.

1.1.4.6 Direct Single Zircon Analysis by TIMS

Nowadays, a high-resolution secondary ion mass spectrometer (HR-SIMS; see Section 4.5.7 and Figure 4.35) is used for the analysis of a spot dating (20–100 μm) by a single zircon using the concordia curve method. Usually, many spots in many zircons are measured to increase the number of data points and to obtain good statistics.

As shown in Figure 1.20, the zircon crystal is not very homogeneous, and contains inclusions (mineral, melt, and fluid), corroded rims, and metamict (amorphous) parts, which are formed by radiation from radioactive U and Th in the zircon itself. Old zircons are often made of an inner core and an outer rim. The inner core inherits the older zircon, which means that there was older granites or older source of the zircon. The outer rim forms the euhedral zircon with corroded and eroded rims. Our targets for age determination are a pure outer rim and an
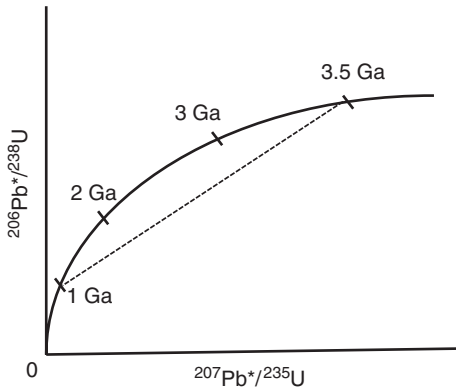
Figure 1.19 Concordia curve. The dotted line indicates a discordia line.
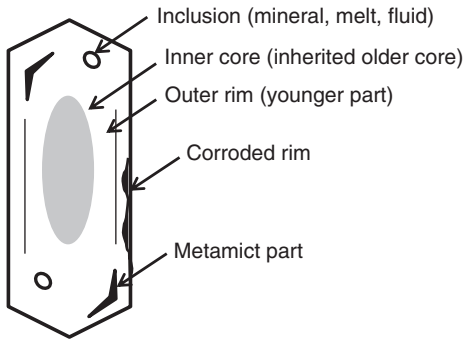
Figure 1.20 Schematic diagram of a zircon crystal.

inner core. In this section, the efforts to obtain accurate ages from a single zircon using (Section 4.5.7 and Figure 4.35) TIMS before HR-SIMS (…) are established are introduced.

Krogh [29] invented the zircon air abrader. In this device, zircons are made to circulate in the metal chamber by air pressure, whereby they are polished as a result of the removal of the corroded rim, inclusions, and metamict parts. By polishing, the common lead is also removed, resulting in higher accuracy in the U−Pb dating. However, when the zircon has an inner core, as shown in Figure 1.20, the age information mainly comes from this core, and data from the outer rim is discarded. However, Aleinikoff *et al.* [30] collected a few micrometer-size dust particles from the zircon abrader and obtained the ages of both the core and the rim.

Kober [31] established a method to obtain the age from a zircon of the closed area for the U−Pb system by TIMS, minimizing the effects from inclusions, amorphous parts, and corroded rims. He used the double Re filament assembly. One

Ionization
filament

Evaporation
filament
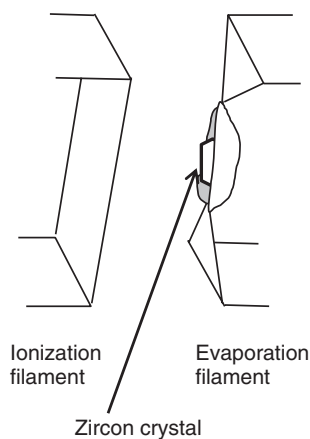
Zircon crystal

Figure 1.21 Double filament assembly for the single zir-
con crystal analysis.

was the normal ionization Re filament and the other was made like a canoe. Then
a single zircon crystal was put in the canoe, and the filament was pinched mak-
ing a window in the direction of the ionization filament (see Figure 1.21). For
measurement, the ionization filament was heated to 1900 °C. Then the evapora-
tion filament was heated. When the evaporation filament temperature was low
(200 – 1200 °C), a weak and unstable Pb ion beam appeared. The isotope ratio
was a mixture of common and radiogenic Pb. When the evaporation filament
temperature was increased to 1350 – 1450 °C, the stable Pb ion beam appeared,
which was measured. This Pb is considered to come from the stable crystalline
phase, and its beam intensity was 10^{-14} A per 1 ng Pb and lasted for 15 – 20 min. As
there was no U data, only the ^{207}Pb/^{206}Pb apparent age (see Eq. (1.48)), which was
the same as the U – Pb crystallization age, was obtained. He concluded that this
method was superior to SIMS (secondary ion mass spectrometry), because the
spatial resolution of SIMS is a few tens of micrometers while that of this method
is 0.1 – 1 µm.

Kober [32] modified this method and obtained a high Pb ionization efficiency
of $0.2 - 1 \times 10^{-3}$. This corresponds to the ionization efficiency of the usual silica
gel – phosphoric acid method. In this method, the unstable Pb was evaporated at
the beginning as in the earlier method [31]. Then the current of the ionization fila-
ment was reduced to 0 A, and the evaporation filament was heated to 1450 °C. The
Pb vapor was deposited on the ionization filament. Then Pb isotope ratios were
measured by heating the evaporation filament to 1150 – 1250 °C. He considered
that Pb/Hf/SiO$_x$ compounds deposited on the ionization filament worked like
Pb/SiO$_2$/PO$_x$ inhibiting the Pb evaporation, resulting in high ionization efficiency
of Pb. He got an error of 30 – 40 Ma (2σ) for the Paleozoic zircons.

Kröner and Todt [33] further modified the method of Kober [32]. They step-
wise heated the evaporation filament from 1400 °C by 20 – 50 °C. In each stage,
the ionization filament temperature was lowered, the sample deposited, and the

filament heated, and the Pb isotope ratio was measured. Then, only the stabilized $^{207}Pb/^{206}Pb$ ratio was used as the age.

1.1.5
Radiogenic Isotopes for Geochemical Tracers

Radiogenic isotopes can be used as tracers in analytical geochemistry. As analytical techniques and mass spectrometer construction improved, radiogenic isotope ratios of $^{87}Sr/^{86}Sr$, $^{143}Nd/^{144}Nd$, $^{206}Pb/^{204}Pb$, $^{207}Pb/^{204}Pb$, $^{208}Pb/^{204}Pb$, $^{187}Os/^{188}Os$, and $^{176}Hf/^{177}Hf$ have been accumulated all over the world, forming a large database. These isotopes are used as $Sr-Nd-Pb-Os-Hf$ isotope tracers. Especially, Pb isotopes are very effective because one element shows three radiogenic isotopes and the mixing line between two components is linear. The isotope ratios $^{87}Sr/^{86}Sr$, $^{206}Pb/^{204}Pb$, $^{207}Pb/^{204}Pb$, $^{208}Pb/^{204}Pb$, and $^{187}Os/^{188}Os$ are generally plotted directly, but $^{143}Nd/^{144}Nd$ and $^{176}Hf/^{177}Hf$ are plotted in ε-notation. The ε-notation is defined as follows:

$$\varepsilon Nd_{sample} = \left[\frac{\left(^{143}Nd/^{144}Nd\right)_{sample}}{\left(^{143}Nd/^{144}Nd\right)_{CHUR}} - 1 \right] \times 10^4 \tag{1.49}$$

$$\varepsilon Hf_{sample} = \left[\frac{\left(^{176}Hf/^{177}Hf\right)_{sample}}{\left(^{176}Hf/^{177}Hf\right)_{CHUR}} - 1 \right] \times 10^4 \tag{1.50}$$

where CHUR stands for "chondritic uniform reservoir." CHUR is the assumed reservoir with Sm/Nd and Lu/Hf ratios of chondrite, so that the isotope ratios $^{143}Nd/^{144}Nd$ and $^{176}Hf/^{177}Hf$ are also those of chondrite.

For Sm/Nd, the measured data are normalized to $^{146}Nd/^{144}Nd = 0.7219$. When $^{143}Nd/^{144}Nd = 0.511860$ for the La Jolla Nd standard (or $^{143}Nd/^{144}Nd = 0.511724$ for the Pheasant Memorial Laboratory (PML) Nd standard), $^{143}Nd/^{144}Nd$ and $^{147}Sm/^{144}Nd$ of CHUR are 0.512638 and 0.1967, respectively.

For Hf, the data are normalized to $^{179}Hf/^{177}Hf = 0.7325$. When $^{176}Hf/^{177}Hf = 0.282147$ for the JMC475 standard (or $^{176}Hf/^{177}Hf = 0.282181$ for the JMC 14 374), $^{176}Hf/^{177}Hf = 0.282772$ is CHUR. The $^{176}Lu/^{177}Hf$ value of CHUR is 0.0334.

In the $Rb-Sr$ case, Rb is very volatile, and therefore the chondritic reservoir cannot be assumed to be that of the bulk silicate earth. Sometimes a "uniform reservoir (UR)" is used like CHUR. As Pb is volatile and can go into the core, how much Pb went into the core or space is unknown. Therefore, isotope ratios are directly used and plotted. Sometimes "geochron" is plotted in the $^{206}Pb/^{204}Pb$ versus $^{207}Pb/^{204}Pb$ isotope plot. This line is an evolution curve of Pb isotope ratios, which starts from the initial Pb isotope ratios of troilite of the Canyon Diablo iron meteorite (CDT) age and various μ-values ($\mu = {}^{238}U/^{204}Pb$). Thus, one geochron is a line with one age (e.g., 4.55, 4.50, and 4.40 Ga, etc.).

In the case of the $Re-Os$ system, both elements are siderophiles (see Figure 1.5), and it is well known that the mantle abundances of PGEs (platinum group elements) are high compared to those of the model of the core formation where

droplets of molten iron accreted to the core with sweeping PGEs from the mantle into the core. After the core formation, the PGE enrichment event should have occurred (the late veneer model). Therefore, PGE of bulk earth has little meaning, and the PUM (primitive upper mantle) isotope ratio and its evolution are sometimes used.

Additionally, stable isotopes such as $^7Li/^6Li$, $^{11}B/^{10}B$, and $^{18}O/^{16}O$ are sometimes plotted against radiogenic $Sr-Nd-Pb-Os-Hf$ isotope tracers. Furthermore, $^{190}Os/^{188}Os$ and $^{138}Ce/^{142}Ce$ are occasionally used. Using these isotopic tracers, we try to decipher what has been occurring from the early solar system to the present dynamic earth through the history of the solar system and earth.

1.2
Element Synthesis in Stars

In this section, the element synthesis in stars is explained because analytical geochemistry sometimes deals with the isotopic anomaly originating from the elemental synthesis in stars. The story of element synthesis starts soon after the Big Bang, the formation of the first stars, and the end of stars (supernovae) in which most elements are synthesized.

1.2.1
Atom, Nucleus, Isotope, and Element

The atom is made of the nucleus and electron(s), which are the same number as protons in the nucleus. The nucleus is made of protons and neutrons, and the mass number is the total number of protons and neutrons. The number of the protons defines the characteristics of the atom, called the *element*. The atom with the same number of protons but with different number of neutrons is called an *isotope*.

The weight of 1 mol of ^{12}C is defined to be exactly 12 u (unified atomic mass unit) or 12 Da (dalton). Previously "amu" (atomic mass unit) was used, but its use is not recommended in the present SI unit system. As the weight of electrons is negligible compared to that of the nucleus, the weight of 1 mol of the nucleus is considered to be the same as the mass number.

1.2.2
Soon after the Big Bang

The universe was formed as a result of the so-called Big Bang at 13.7 Gyr. Inflation theory predicts that the universe was formed from nothing to almost the present size within a second. After the inflation, the universe became cool enough for the proton (hydrogen) and neutron to exist. ^1H and neutron (^1n) produced the deuterium (^2H); deuterium and neutron produced tritium (^3H); the tritium decayed into ^3He; and ^3He and a neutron produced ^4He.
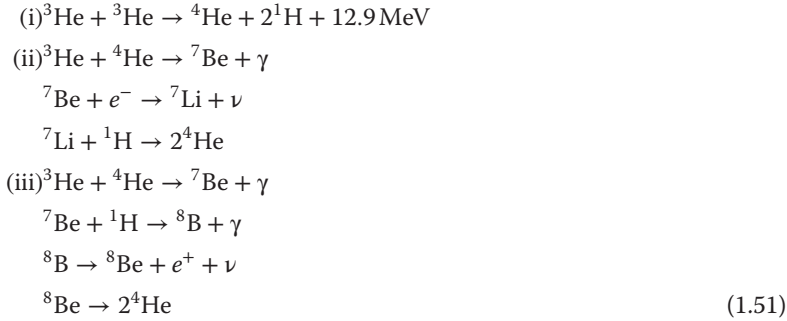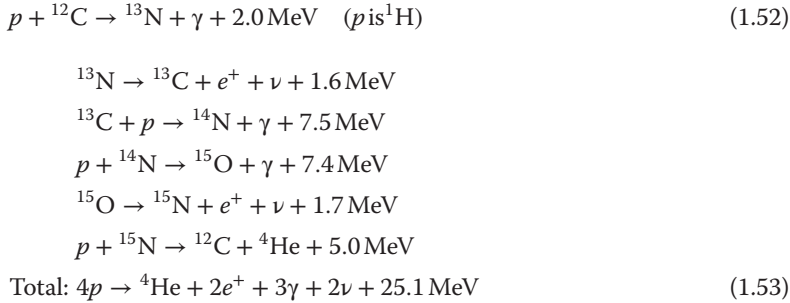
1.2.3
Element Synthesis in Stars

The first stars appeared 0.55 Gyr after the Big Bang, and then the heavier elements were formed in stars. The core of the star is sustained by balances of three forces: (i) energy produced by nuclear reaction, (ii) gravity by the huge body, and (iii) repulsion by electron degeneration.

At the beginning of a star, ^{3}He and ^{1}H burn to make ^{4}He. There are two paths of this reaction: the proton–proton chain reaction, and the CNO cycle.

In the proton–proton reaction, ^{1}H $+\,^1$H $\rightarrow\,^2$H $+ e^+ +$ neutrino occurs, and $e^+ + e^- \rightarrow 1.0$ MeV occurs, and energy is produced. Then ^{2}H $+\,^1$H $\rightarrow\,^3$He $+ 5.5$ MeV occurs. Then three branches occur:

$$(\text{i})^3\text{He} +\,^3\text{He} \rightarrow\,^4\text{He} + 2^1\text{H} + 12.9\,\text{MeV}$$

$$(\text{ii})^3\text{He} +\,^4\text{He} \rightarrow\,^7\text{Be} + \gamma$$

$$^7\text{Be} + e^- \rightarrow\,^7\text{Li} + \nu$$

$$^7\text{Li} +\,^1\text{H} \rightarrow 2^4\text{He}$$

$$(\text{iii})^3\text{He} +\,^4\text{He} \rightarrow\,^7\text{Be} + \gamma$$

$$^7\text{Be} +\,^1\text{H} \rightarrow\,^8\text{B} + \gamma$$

$$^8\text{B} \rightarrow\,^8\text{Be} + e^+ + \nu$$

$$^8\text{Be} \rightarrow 2^4\text{He} \tag{1.51}$$

Another reaction is the CNO cycle:

$$p +\,^{12}\text{C} \rightarrow\,^{13}\text{N} + \gamma + 2.0\,\text{MeV} \quad (p\,\text{is}\,^1\text{H}) \tag{1.52}$$

$$^{13}\text{N} \rightarrow\,^{13}\text{C} + e^+ + \nu + 1.6\,\text{MeV}$$

$$^{13}\text{C} + p \rightarrow\,^{14}\text{N} + \gamma + 7.5\,\text{MeV}$$

$$p +\,^{14}\text{N} \rightarrow\,^{15}\text{O} + \gamma + 7.4\,\text{MeV}$$

$$^{15}\text{O} \rightarrow\,^{15}\text{N} + e^+ + \nu + 1.7\,\text{MeV}$$

$$p +\,^{15}\text{N} \rightarrow\,^{12}\text{C} +\,^4\text{He} + 5.0\,\text{MeV}$$

$$\text{Total:}\ 4p \rightarrow\,^4\text{He} + 2e^+ + 3\gamma + 2\nu + 25.1\,\text{MeV} \tag{1.53}$$

However, these reactions alone cannot make heavier elements. The core of an old star is rich in ^{4}He, and the temperature is >100 MK. In this condition, the triple-alpha process can occur:

$$^4\text{He} +\,^4\text{He} \rightarrow\,^8\text{Be} + \gamma - 91.8\,\text{keV} \tag{1.54}$$

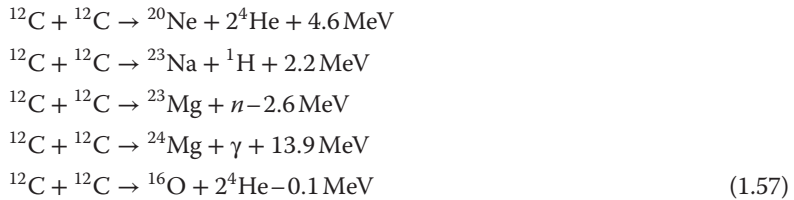$$^8\text{Be} +\,^4\text{He} \rightarrow\,^{12}\text{C} + \gamma + 7.4\,\text{MeV} \tag{1.55}$$

Totally, 7.3 MeV is generated. ^{8}Be is very unstable, and returns to two ^{4}He in 2.6×10^{-16} s. However, in the condition under which He burns, this reaction becomes an equilibrium reaction. In addition, the energy of the second reaction

is almost the same as the exited state of ^{12}C. Therefore, these two rare reactions occur. At the same time, oxygen atoms are formed:

$$^{12}\text{C} + {}^{4}\text{He} \rightarrow {}^{16}\text{O} + \gamma \tag{1.56}$$

However, the next reaction forming ^{20}Ne does not occur because of the restriction from the nuclear spin. In 1957, Burbidge, Burbidge, Fouler, and Hoyle published a famous B^{2}FH theory [34]. In this theory, heavier elements are made by C-burning, Ne-burning, O-burning, Si-burning, the s-process, the r-process, and the p-process.
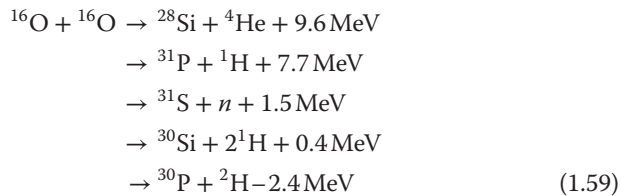
In C-burning, the following reactions occur, and the first two reactions are the main ones.

$$^{12}\text{C} + {}^{12}\text{C} \rightarrow {}^{20}\text{Ne} + 2{}^{4}\text{He} + 4.6\,\text{MeV}$$
$$^{12}\text{C} + {}^{12}\text{C} \rightarrow {}^{23}\text{Na} + {}^{1}\text{H} + 2.2\,\text{MeV}$$
$$^{12}\text{C} + {}^{12}\text{C} \rightarrow {}^{23}\text{Mg} + n - 2.6\,\text{MeV}$$
$$^{12}\text{C} + {}^{12}\text{C} \rightarrow {}^{24}\text{Mg} + \gamma + 13.9\,\text{MeV}$$
$$^{12}\text{C} + {}^{12}\text{C} \rightarrow {}^{16}\text{O} + 2{}^{4}\text{He} - 0.1\,\text{MeV} \tag{1.57}$$

After C-burning and C is consumed, Ne-burning occurs. Higher pressure and temperature are required for Ne-burning. In such high temperatures, photodisintegration cannot be ignored (the first reaction), and part of the Ne nuclei decay. In a few years, Ne is consumed in the core of the star, and the core becomes unstable, made of O and Mg.

$$^{20}\text{Ne} + \gamma \rightarrow {}^{16}\text{O} + {}^{4}\text{He}$$
$$^{20}\text{Ne} + {}^{4}\text{He} \rightarrow {}^{24}\text{Mg} + \gamma \tag{1.58}$$

The O-burning process starts after Ne is consumed.

$$^{16}\text{O} + {}^{16}\text{O} \rightarrow {}^{28}\text{Si} + {}^{4}\text{He} + 9.6\,\text{MeV}$$
$$\rightarrow {}^{31}\text{P} + {}^{1}\text{H} + 7.7\,\text{MeV}$$
$$\rightarrow {}^{31}\text{S} + n + 1.5\,\text{MeV}$$
$$\rightarrow {}^{30}\text{Si} + 2{}^{1}\text{H} + 0.4\,\text{MeV}$$
$$\rightarrow {}^{30}\text{P} + {}^{2}\text{H} - 2.4\,\text{MeV} \tag{1.59}$$

In this process, the core of the star becomes Si-rich, but the temperature is not enough to ignite Si. After all O is consumed, Si-burning starts. At this time, from the inside, O-burning shell, Ne-shell, C-shell, He-shell, and H-shell exist like onion shells.

The star with <3 solar masses finishes just after all H becomes He.
The star with 3−8 solar masses dies after He-burning, leaving the C core.
The star with 8−11 solar masses can burn C, and finally become Si.

Si-burning is a process that occurs in a massive giant star with >8−11 times the solar mass. This process is just a 2-week-long process, and then the star becomes a

type-II supernova. The Si-burning processes produce new elements in sequence, and ends making ^{56}Ni within a day.

$$^{28}\text{Si} + {}^{4}\text{He} \rightarrow {}^{32}\text{S}$$

$$^{32}\text{S} + {}^{4}\text{He} \rightarrow {}^{36}\text{Ar}$$

$$^{36}\text{Ar} + {}^{4}\text{He} \rightarrow {}^{40}\text{Ca}$$

$$^{40}\text{Ca} + {}^{4}\text{He} \rightarrow {}^{44}\text{Ti}$$

$$^{44}\text{Ti} + {}^{4}\text{He} \rightarrow {}^{48}\text{Cr}$$

$$^{48}\text{Cr} + {}^{4}\text{He} \rightarrow {}^{52}\text{Fe}$$

$$^{52}\text{Fe} + {}^{4}\text{He} \rightarrow {}^{56}\text{Ni} \tag{1.60}$$

This reaction stops and does not go to ^{60}Zn, because ^{56}Ni is the most stable nucleus. ^{56}Ni decays to ^{56}Co by β^+-decay, and ^{56}Co decays to ^{56}Fe also by β^+-decay. The core supports huge gravity by the energy produced by the nuclear reaction. However, when the iron core is formed, there is no energy to support the core against gravity. Then the core of the star suddenly collapses. As the core collapses, the temperature increases, producing high-energy gamma rays. The gamma rays cause photodisintegration of ^{56}Fe because the following reaction occurs:

$$^{56}\text{Fe} + \gamma \rightarrow 13\,{}^{4}\text{He} + 4n \tag{1.61}$$

This reaction is endothermic, so the core collapses at once. Then, by the shock wave of the collapse the star explodes. This is type-II supernova.

In the explosion, when the repulsion of electrons is overwhelmed by the explosion, the nuclei become neutrons, and the core becomes a neutron star. When the mass is large, the core becomes not a neutron star but a black hole.

1.2.4
Element Syntheses in Other Processes

1.2.4.1   The r-Process

In the previous section, we showed how elements lighter than Fe are formed. In type-II supernova, the r-process occurs ("r" stands for "rapid"). It is believed that when a type-II supernova occurs, a very neutron-rich condition happens before the element decays by β^--decay. Thus neutron-rich elements are formed at once. Then unstable neutron-rich isotopes decay to stable isotopes through β^--decay.

1.2.4.2   The p-Process

In the type-II supernova, the very strong light (photons) is also generated, which breaks the nuclei. This photodisintegration process is called the *p-process*. The p-process was required to make proton-rich isotopes in the B^{2}FH theory, which cannot be generated by either the r-process or the s-process (see Section 1.2.4.3). In the early theory, "p" meant "proton-rich," but now it means "photodisintegration." There are not many p-isotopes.
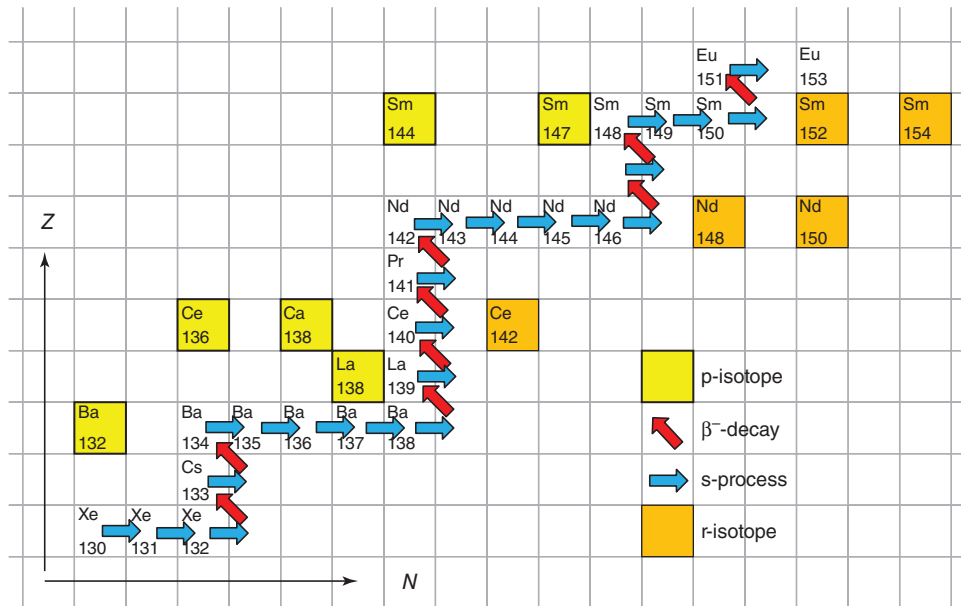
1.2.4.3 The s-Process

The s-process is considered to form neutron-rich nuclei "slowly" in thousands of years, and occurs in AGB star (asymptotic giant branch) star or stars with low metallicity. The seed is C, and neutrons are supplied by the following reactions:

$$^{13}C + {}^{4}He \rightarrow {}^{16}O + n \tag{1.62}$$

$$^{12}C + {}^{12}C \rightarrow {}^{23}Mg + n \tag{1.63}$$

Neutron-rich isotopes of proton number Z are formed by the s-process ($N + 1$, $N + 2$, $N + 3$, ...), and finally a short-half-life isotope appears, ends by β^--decay, and then goes up to the next element, $Z + 1$. This process goes up to Bi. For example, formation of elements from Xe to Eu by the s-process is shown in Figure 1.22. The horizontal blue arrow indicates the s-process, and the red slanted arrow indicates β^--decay. The isotopes in yellow and orange boxes show the p- and r-isotopes, respectively. Some isotopic anomalies of the s-process isotopes are found in the pre-solar grains, which are micrometer-size particles contained in primitive carbonaceous chondrites.

1.2.4.4 The x-Process

In B^{2}FH theory, Li, Be, and B were not synthesized, and their low abundances could not be explained. Thus they were named, and considered to be formed

Figure 1.22 Formation of elements from Xe to Eu by the s-process. The horizontal and vertical axes indicate numbers of neutrons and protons in a nucleus, respectively.

by, the x-process. They are now considered to be synthesized by spallation by high-energy galactic cosmic rays. This is the reason why the solar abundances of Li, Be, and B are very low. However, recently Tajitsu *et al.* [35] observed ^{7}Be in a carbon−oxygen supernova for the first time, formed by a ^{3}He$(\alpha,\gamma)^7$Be reaction, which will produce ^{7}Li by ^{7}Be$(e^-,\nu)^7$Li. Therefore, Li will be produced in the usual supernova. (AM: It is exciting that isotopes of faraway supernovae can be detected by improvement of the observatory and spectrometers in astronomy *without* using mass spectrometers!)

1.2.4.5   Type Ia Supernova

Chandrasekhar calculated the limit of the mass of a white dwarf. He concluded that if the mass of a white dwarf becomes 1.26 times that of the sun (it is called as the *Chandrasekhar limit*), electron degeneration cannot hold the gravity, and the white dwarf should explode and could become a neutron star. Such a supernova is called a type-Ia supernova.

In the previous section, we mentioned that a star of <3 solar masses will die after the H and He fuels are consumed. The gravity balances the repulsion of electron degeneration because of the small masses. The star becomes a white dwarf and cooler. However, there is a possibility that the white dwarf is composed of twin stars. In such a case, gases of a companion star can gather on the white dwarf and explode on the white dwarf by exceeding the Chandrasekhar limit. This is type-Ia supernova.

1.2.5
Other Types of Supernovae

When a supernova is observed, it is classified by its spectrum. If the absorption spectrum of H is observed, it is classified as type-II. Type-I has no absorption spectrum of H because most H would have been consumed by the white dwarf.

There are three subtypes of type-I supernovae: type-Ia, type-Ib, and type-Ic. Type-Ib and type-Ic lack the 635.5 nm absorption of Si. In addition, as time passes, the spectrum of type-Ia is composed of the absorption line of Fe, while type-Ib and type-Ic show those of O, Ca, and Mg. The type-Ic lacks the 587.6 nm absorption of He, but in type-Ib it is present. Origins of the type-Ib, type-Ic, and type-II are similar, and are called *stripped core-collapse supernovae.* Type-Ib is a star of large mass with the onion shell structure, but H is stripped by a companion star. Type-Ic is also a large-mass star, but H and He are stripped by a companion star.

1.3
Errors

In this section, the basics of errors are explained. As more than 100 isotopic ratios are measured for one sample in TIMS, the statistics are important. (AM: However, the used statistics is very simple.)

1.3.1
Average and Standard Deviation

Here, we assume the simplest case. When there is one standard solution, the solution is loaded on the filament separately and measured automatically based on the same method. We get the first analytical value (A_1), the second value (A_2), ..., nth value (A_n) by the same method with the same analytical condition in a short time. Then we obtain the average (B) as

$$B = (A_1 + A_2 + \cdots + A_n)/n \tag{1.64}$$

The standard deviation (sometimes denoted as SD or σ) is obtained as

$$\mathrm{SD} = \left(\sum (Ai - B)^2/(n-1) \right)^{1/2} \tag{1.65}$$

which is easily obtained by a "STDEV" function in the Microsoft® EXCEL® worksheet.

We can calculate the relative standard deviation percentage (RSD%) as

$$\mathrm{RSD\%} = \mathrm{SD}/B \times 100 \tag{1.66}$$

2 RSD% means twofold RSD%.

We call SD of the same sample in short time (e.g., the repeated measurements of the same sample) as "repeatability", and *not* as "precision."

We use "intermediate precision", but *not* "reproducibility or repeatability," which is obtained from measurements of the same sample but starting from the different sample digestions.

These usages are the present ISO (International Standard Organization) suggestions (~2011). (AM: Not because the author is a non-native English speaker!) The old "precision" and "reproducibility" need to be called *repeatability* and *intermediate precision*. A summary is given in Table 1.5 and Section 1.3.4. These expressions are uniformly used in this book (which is written in 2014–2015). Details are explained in Section 1.3.4.

Table 1.5 The summary of the old and new (ISO) usages of the words.

| Old usage	New ISO usage
Precision	Repeatability
Reproducibility, repeatability (intra-laboratory variation)	Intermediate precision
Inter-laboratory variation	Reproducibility
Accuracy (total error including repeatability and difference from the true value)	Accuracy (precision) (total error including repeatability and difference from the true value)
Trueness	Trueness
True value (AM: only God knows!)	True value
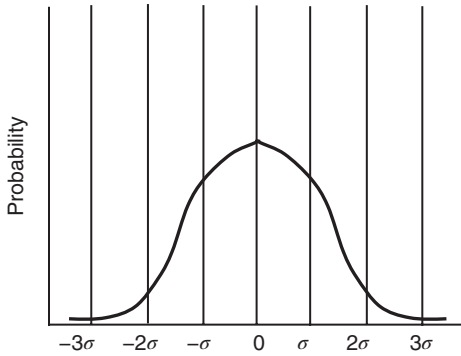
Figure 1.23 Normal distribution.

1.3.2
Normal Population

The normal population is one of ideal variations of data. As shown in Figure 1.23, the data points are scattered, forming a bell shaped curve. The horizontal axis is the data value, and the vertical axis is the probability. When this curve is integrated from $-\infty$ to $+\infty$, the integrated probability becomes 1. From $-\sigma$ to $+\sigma$, 68.3% of the data are included. From -2σ to $+2\sigma$, 95.4% of the data are included. From -3σ to $+3\sigma$, 99.7% of the data are included. This distribution is expressed as

$$y = \exp[-1/2[(x - B)/\sigma]^2]/[\sigma(2\pi)^{1/2}] \tag{1.67}$$

where B is the average and σ is the standard deviation.

1.3.3
Standard Error

We assume a normal population with an average B and a standard deviation σ. Then we randomly take n samples, and make a subpopulation. What we want to do is to estimate the average and standard deviation of the parent population from the subpopulation.

The average and the standard deviation of the subpopulation are B' and SE (standard error). From the statistics, $B = B'$. The standard deviation of the subpopulation, SE, is called the *standard error*. The standard error should be

$$SE = SD/n^{1/2} \tag{1.68}$$

In other words, the probability that the estimated B is within the range $B \pm SE$ is 0.68. $B \pm 1.96SE$ is 0.95 and $B \pm 2.85SE$ is 0.99. In isotope ratio measurement, >100 ratios are measured as subpopulation, and the standard error is used as the error. Thus the standard deviations of obtained ratios are divided by $n^{1/2}$, and the error of one measurement is presented as SE.

1.3.4
ISO Suggestion

In this book, two types of errors are used: repeatability and intermediate precision, because ISO redefined these words. We used "precision" ("indicates old usage"), but this should be called *repeatability*. Now, ISO's precision is almost similar to what was previously called *accuracy*, which includes the difference from the true value.

Intermediate precision is, when the sample is a homogeneous powder, the error of repeated measurements starting from digesting the sample. "Repeatability" or "reproducibility" was used for this term. Now, reproducibility has a different meaning, namely the difference among laboratories. As we do not know the true value, intermediate precision is used to evaluate the accuracy. Both definitions are randomly used even in analytical chemistry papers. Therefore, care should be taken when you read or write papers. In Table 1.5, a summary is given.

"Error" and "uncertainty" are vague terms, which sometimes express repeatability and sometimes mean intermediate precision or accuracy. They sometimes indicate RSD and sometimes 2RSD%. Therefore, we must be careful, and clarify the definition, when we use "error" or "uncertainty."

1.3.5
Modified Savitzky–Golay Method

Gorry [36] presented a simple data-fitting method. This method solved the problem whereby $(2m + 1)$ data become $2m$ data after fitting. This method, the modified Savitzky–Golay method, is a simple function in five-point quadratic smoothing, given by

$$Y_2 = (3y_{-2} - 5y_{-1} - 3y_0 + 9y_1 + 31y_2)/35$$
$$Y_1 = (-5y_{-2} + 6y_{-1} + 12y_0 + 13y_1 + 9y_2)/35$$
$$Y_0 = (-3y_{-2} + 12y_{-1} + 17y_0 + 12y_1 - 3y_2)/35$$
$$Y_{-1} = (9y_{-2} + 13y_{-1} + 12y_0 + 6y_1 - 5y_2)/35$$
$$Y_{-2} = (31y_{-2} + 9y_{-1} - 3y_0 - 5y_1 + 3y_2)/35 \tag{1.69}$$

where the raw data is y_n and fitted data are Y_n. The raw data ends at y_2, and the fitted data ends at Y_2. Thus all the points can be smoothed without loss of data.

1.3.6
Variance, Covariance, and Correlation Coefficient

We assume there are two variables (x, y) and a series of paired values (x_1, y_1), $(x_2, y_2), \ldots, (x_N, y_N)$. For example, these data can be from a couple of analyses of two isotopic or chemical ratios. We can calculate the means for both variables:

$$Y = \left(\sum y_i \right) / N \tag{1.70}$$

$$X = \left(\sum x_i \right) / N \tag{1.71}$$

We can define the variances of x and y as

$$V_y = \sum (y_i - Y)^2 / N \tag{1.72}$$

$$V_x = \sum (x_i - X)^2 / N \tag{1.73}$$

The standard deviations, which are the square roots of the variances, are obtained as

$$\sigma_y = \sqrt{V_y} = \sqrt{\left[\sum (y_i - Y)^2 / N \right]} \tag{1.74}$$

$$\sigma_x = \sqrt{V_x} = \sqrt{\left[\sum (x_i - X)^2 / N \right]} \tag{1.75}$$

The covariance is defined as

$$V_{yx} = V_{xy} = \sum (y_i - Y)(x_i - X) / N \tag{1.76}$$

The covariance is an index that shows the correlation between y and x. If there is no correlation, the covariance is 0. If positive or negative correlations exist, the covariance becomes positive or negative, respectively. To make the covariance free from the units of y and x, the correlation coefficient, r, is introduced:

$$r = V_{yx} / \sqrt{(V_{xx} V_{yy})} = \sum (y_i - Y)(x_i - X) / \sqrt{\sum (y_i - Y)^2} \sqrt{\sum (x_i - X)^2} \tag{1.77}$$

When there is no correlation between y and x, $r = 0$; when y and x are fully positively correlated, $r = 1$; and when they are fully negatively correlated, $r = -1$. Usually, we take it that when $|r| > 0.90$ there is a correlation between y and x. If $|r| < 0.90$, there is poor correlation between y and x.

1.3.7
Weighted Average, Variance, and Covariance

When we take the uncertainty of each data point into account, the weighted average is calculated as

$$X_\sigma = \frac{\sum (x_i / \sigma_i^2)}{\sum (1 / \sigma_i^2)} \tag{1.78}$$

The variance and covariance are analogously calculated as

$$V_x = \frac{\sum ((x_i - X_\sigma)^2 / \sigma_i^2 / (N - 1))}{\sum (1 / \sigma_i^2) / N} \tag{1.79}$$

$$V_{yx} = \frac{\sum ((y_i - Y_\sigma)(x_i - X_\sigma) / \sigma_i^2) / (N - 1)}{\sum (1 / \sigma_i^2) / N} \tag{1.80}$$

1.3.8
The Least-Squares Method

Assume there are (x, y) datasets as Section 1.3.6 and they are fitted by the straight line $y = ax + b$. The usual criterion is to minimize the distance between the points and the line. The distance D is written as

$$D^2 = (y_1 - b - ax_1)^2 + (y_2 - b - ax_2)^2 + \cdots + (y_N - b - ax_N)^2 \qquad (1.81)$$

We try to minimize the distance from two unknown parameters a and b. We therefore can write

$$\partial(D^2)/\partial a = 0 = \sum -2x_i(y_i - b - ax_i) \qquad (1.82)$$

$$\partial(D^2)/\partial b = 0 = \sum -2(y_i - b - ax_i) \qquad (1.83)$$

The solutions are

$$a = Y - rX\sigma_y/\sigma_x \qquad (1.84)$$

$$b = r\sigma_y/\sigma_x \qquad (1.85)$$

where r is the correlation coefficient given by Eq. (1.77). Then the equation of the best straight line fit is

$$y = Yx - r\sigma_y/\sigma_x(Xx - 1) \qquad (1.86)$$

The uncertainty on the slope (p) is

$$(p) = \sigma_y\sqrt{(1 - r^2)}/[\sigma_x\sqrt{N}] \qquad (1.87)$$

The uncertainty on the ordinate at the origin (I) is

$$(I) = \sigma_x\sqrt{(1 - r^2)}/[\sigma_y\sqrt{N}] \qquad (1.88)$$

However, these solutions do not include the uncertainty of each data. To include them, sophisticated mathematics is required. They are described in York [28] and included in the program package ISOPLOT by Ludwig [37] and later versions.